THE ENDOSYMBIOTIC GUT FUNGUS *ZANCUDOMYCES CULISETAE* INFLUENCES TRANSSTADIAL TRANSMISSION OF HOST-ASSOCIATED MICROBIOTA IN THE YELLOW FEVER MOSQUITO (*AEDES AEGYPTI*)

by

Jonas Frankel-Bricker

A thesis

submitted in partial fulfillment

of the requirements for the degree of

Master of Science in Biology

Boise State University

May 2019

BOISE STATE UNIVERSITY GRADUATE COLLEGE

DEFENSE COMMITTEE AND FINAL READING APPROVALS

of the thesis submitted by

Jonas Frankel-Bricker

Thesis Title: The Endosymbiotic Gut Fungus *Zancudomyces culisetae* Influences Transstadial Transmission of Host-Associated Microbiota in the Yellow Fever Mosquito (*Aedes aegypti*)

Date of Final Oral Examination: 4 March 2019

The following individuals read and discussed the thesis submitted by student Jonas Frankel-Bricker, and they evaluated the student's presentation and response to questions during the final oral examination. They found that the student passed the final oral examination.

Merlin M. White, Ph.D.	Chair, Supervisory Committee
Sven Buerki, Ph.D.	Member, Supervisory Committee
Kevin Feris, Ph.D.	Member, Supervisory Committee

The final reading approval of the thesis was granted by Merlin White, Ph.D., Chair of the Supervisory Committee. The thesis was approved by the Graduate College.

ACKNOWLEDGEMENTS

This project was supported by Institutional Development Awards (IDeA) from the National Institute of General Medical Sciences of the National Institutes of Health under Grants #P20GM103408 (Idaho INBRE) and #P20GM109095 (Idaho COBRE), the Robert W. Lichtwardt Student Research Award from the Mycological Society of America, a College of Arts and Sciences Award from Boise State University, and NSF grant DEB 1441677. All sequencing data collection and preliminary analyses performed by the IBEST Genomics Resources Core at the University of Idaho were supported in part by NIH COBRE grant #P30GM103324. I would like to thank Dr. Sven Buerki, Dr. Kevin Feris, and Dr. Merlin White for serving on my committee and providing continued guidance and support throughout the duration of this project. Special thanks to Laura Bond for her expertise and advice regarding the statistical analyses conducted, to Mick Song for continued collaboration on multiple research projects past and present, and to Michael Wohjahn for instruction and recommendations for coding in R. Finally, thank you to our collaborators at the University of Idaho Genomics Resources Core: Sam Hunter, Matt Fagnan, and especially Dan New for their knowledge and support throughout the next generation sequencing workflow.

ABSTRACT

Mosquitoes are vectors for a variety of human pathogens and have a significant impact on human health worldwide. There is growing evidence that host-associated microbiota influence mosquito vector competence for certain viruses. Transstadial transmission of bacteria from larvae through pupae to adults could affect these interactions, though further studies are needed to fully unravel the mechanisms involved. Current microbiome research primarily focuses on bacterial communities, whereas the potential role endosymbiotic gut fungi have in transstadial transmission dynamics remains largely unknown. Trichomycetes is an ecological group of endosymbiotic microfungi that colonize the digestive tracts of arthropod hosts, including the Yellow Fever Mosquito (*Aedes aegypti*). The trichomycete fungus *Zancudomyces culisetae* infects *A. aegypti* populations in the wild and was investigated using laboratory-based assays to identify fungal-bacterial-host interactions in mosquito larvae and adults.

Next generation sequencing of 16S rDNA gene amplicons and measures of microbiome diversity found that fungal infestation in the larval digestive tract influenced their microbiomes and reduced microbial transstadial transmission variability. Comparative analyses of beta diversity measures indicated that fungal infestation affected larval microbiome composition. Measures of alpha diversity revealed that newly emerged fungal adults contained microbiomes characterized by high bacterial diversity and even community distributions. In contrast, non-fungal adults harbored microbiomes with variable compositional structures, often with low bacterial diversity and high levels of

dominance by few taxa. Additionally, transstadial transmission processes impacted certain bacterial families. Fungal infestation in larvae restricted the transmission and establishment of the bacterial taxon *Burkholderiaceae* and increased relative abundance of *Corynebacteriaceae* and *Moraxellaceae* in newly emerged adults. Identifying biotic factors that interact with host-associated microbiota and contribute to adult microbiome formation may reveal microbial interactions that affect human pathogen contraction and transmission in mosquitoes. These findings emphasize the importance of accounting for endosymbiotic gut fungi in host-associated microbiome studies.

TABLE OF CONTENTS

LIST OF TABLES

LIST OF FIGURES

LIST OF ABBREVIATIONS

BHI	Brain Heart Infusion
CDC	The Centers for Disease Control and Prevention
CV	Coefficient of Variation
FLASH	Fast Length Adjustment of Short Reads
G	Gravity
GRC	Genomics Resources Core
MSLRT	Modified Signed Likelihood Ratio Test
NMDS	Non-Metric Multidimensional Scaling
PCR	Polymerase Chain Reaction
PERMANOVA	Permutational Analysis of Variance
OUT	Operational Taxonomic Unit
SCML	Spike-in Calibration to Microbial Load
USDA-ARS	United States Department of Agriculture- Agricultural Research Service

INTRODUCTION

Arthropods coexist with communities of microbes collectively referred to as a microbiome. Mosquitoes have become target organisms for microbiome studies due to their vast geographic ranges (Kraemer et al., 2015) and high vector competence for a variety of human pathogens according to the CDC. They are holometabolous, developing from eggs to larvae and then forming pupae in aquatic environments, later to emerge as flying terrestrial adults. These life history traits provide a system for the observation and study of microbiomes across developmental stages in an organism prevalent in ecosystems worldwide and associated with significant human health concerns.

Mosquito-associated microbiota have been studied in larvae (Rani et al., 2009; Duguma et al., 2013; Coon et al., 2014), adults (Rani et al., 2009; Gusmão et al., 2010; Chandler et al., 2015; Dickson et al., 2018), and compared across mosquito species (Zouache et al., 2011; Coon et al., 2014; Muturi et al., 2016b; Muturi at al., 2017). Microbial communities can impact larval development (Chouaia et al., 2012; Coon et al., 2014), affect adult fitness (Minard et al., 2013), and play a role in the key processes related to blood digestion and egg production (Gaio et al., 2011; Coon et al., 2016). Adult microbiomes also influence mosquito-human pathogen interactions (Dennison et al., 2014), which can change host vector competence for malarial parasites (Dong et al., 2009) and arboviruses (Ramirez et al., 2012; Jupatanakul et al., 2014; Hegde et al., 2015; Carissimo et al., 2015). Certain bacterial genera, including *Wolbachia* (Bian et al., 2010; Pan et al., 2012; Bourtzis et al., 2014), *Chromobacterium* (Ramirez et al., 2014), and

Serratia (Apte-Deshpande et al., 2012) contribute to differential host-pathogen interactions, and vector competence can vary across different populations of the same mosquito species (Charan et al., 2013; Gonçalves et al., 2014). Additionally, gut microbiomes change compositionally in response to temporal shifts of pathogen exposure (Novakova et al., 2017) and after contraction (Zink et al., 2015). The significant microbial interactions impacting mosquito vector competence motivate continued research into factors that influence adult gut microbiome composition, structure, and function.

Larval microbiome dynamics have impacts on adults. Native larval gut microbiomes impede vertical transmission of *Wolbachia* (Hughes et al., 2014), whereas successful establishment of this genus in larvae impacts microbiome structure in adults (Audsley et al., 2018). Additionally, larval exposure to various environmental bacteria alters adult susceptibility to pathogen contraction (Dickson et al., 2017). Investigating the processes that contribute to these developmental stage microbe inter-relationships provide insights regarding the extent to which larval and adult microbiomes are connected.

A source for initial adult microbe acquisition is via bacteria transferred through preceding larval and pupal stages. Certain bacterial taxa present in larvae are transstadially transmitted and found in adults (Wang et al., 2011; Coon et al., 2014; Chen et al., 2015; Duguma et al., 2015). However, adults and larvae harbor microbiomes that differ in composition and structure (Wang et al., 2011; Gimonneau et al., 2014; Duguma et al., 2015), indicating that processes during life stage transitions and disparate phenotypic traits result in distinct bacterial communities. Importantly, morphological and

physiological mechanisms reduce the bacterial load in mosquito digestive tracts during and after pupation (Moll et al., 2001; Moncayo et al., 2005). It is unclear how transstadially transmitted taxa establish in adult digestive tracts after this process. One explanation is that these microbes are not expelled because they inhabit other anatomical parts of the larval host that are not shed during pupation, such as the hemocoel (Brown et al., 2018) and the salivary glands (Sharma et al., 2014). Whether these communities establish in adult digestive tracts after pupation is uncertain. However, certain bacteria colonize the digestive tracts and malpighian tubules in larvae, are transstadially transmitted through the malpighian tubules, and reestablish in newly emerged adult digestive tracts (Chavshin et al., 2013; Chavshin et al., 2015). Research that analyzes mechanisms which influence the microbiome transition across developmental stages is crucial to further our understanding of how adult gut microbiomes form and influence vector competence.

The quantity of bacteria in a microbiome could affect microbe-host dynamics. Novel protocols have been developed that add controlled amounts of nonnative bacteria (Smets et al., 2016; Stämmler et al., 2016) to experimental samples prior to sequencing, and are more accurate than qPCR when quantifying entire bacterial communities (Stämmler et al., 2016). SCML (Stämmler et al., 2016) is a protocol that clarifies whether observed taxonomic shifts in relative abundance are due to increased proliferation or to differential die-off of certain bacterial taxa within a microbiome.

Many microbiome studies assess bacteria and archaea, however, mosquitoes also harbor communities of fungi (Chandler et al., 2015; Muturi et al., 2016b) which can impact host fitness and interact with gut microbiota. Several entomopathogenic fungi

decrease bacterial diversity, accelerate death rates in adults (Wei et al., 2017), and affect gut bacterial load (Ramirez et al., 2018). Additionally, an endosymbiotic fungus increased vector competence for the dengue virus in adults and inhibited growth of certain gut bacterial taxa (Angleró-Rodríguez et al., 2017). These studies reveal important fungal-bacterial-host dynamics in adults, but are understudied in larvae. To the best of our knowledge, the potential impacts of endosymbiotic gut fungi on transstadial transmission of host-associated microbiota have never been addressed.

Trichomycetes include a group of microfungi that are obligate endosymbionts of certain larval, aquatic arthropods (Lichtwardt, 1986). *Zancudomyces culisetae*, a well-studied member of the Harpellales, infests the hindguts of several dipteran hosts (Williams and Lichtwardt, 1972; Lichtwardt 1984). Asexual fungal spores in the aquatic environment are ingested by larvae, extrude sporangiospores that attach to the lining of the digestive tract in response to physiological cues, and develop in the hindgut. Experimental fungal infestation assays have allowed for the study of these mechanisms (Williams, 1983; Horn, 1989; McCreadie and Beard, 2003; Vojvodic and McCreadie, 2007). Whereas the nature of this fungal-host relationship is presumed to be commensalistic, it can shift towards mutualism under altered environmental conditions (McCreadie et al., 2005). The Yellow Fever Mosquito (*Aedes aegypti*), a vector for the human pathogens Yellow, Dengue, Chikungunya, and Zika fevers, is one of the known hosts of *Z. culisetae* in nature (Alencar et al., 2003). If this gut fungus affects *A. aegypti* microbiome dynamics, wild populations could experience distinct host-microbiome interactions contingent on the presence of *Z. culisetae* in their local environment, which may lead to differential vector competence across mosquito populations.

To investigate fungal-bacterial-host interactions across developmental stages, *A. aegypti* larvae were experimentally infected with *Z. culisetae* in a controlled laboratory environment. Microbiomes of larvae and newly emerged adults were analyzed with 16S rDNA gene amplicon sequencing and comparative metagenomic analyses to identify potential changes in transstadial transmission patterns and shifts in newly emerged adult microbiome compositional structures influenced by fungal infestation of the larval digestive tract.

Materials and Methods

Fungal Strain Culturing and Spore Collection

A culture of *Z. culisetae* (USDA-ARS Collection of Entomopathogenic Fungal Cultures, Ithaca, New York, USA, ARSEF 9012, *Smittium culisetae*, COL-18-3) was maintained at room temperature on a 1/10 BHI agar plate with 3 milliliters (ml) autoclaved Nanopure Water (Barnstead Thermolyne Corp., Dubuque, IA, USA) overlay containing 2 milligrams (mg)/ml of penicillin and 7mg/ml of streptomycin to prevent bacterial contamination. Fungal mycelia were transferred to a new 1/10 BHI agar plate with 3ml autoclaved Nanopure Water 8 days prior to the start of the experiment.

Fungal spores were harvested at the start of the experiment by sterilely collecting and filtering the overlay through a sheet of Miracloth® (EMD Millipore, Burlington, MA, USA) with a pore size of 22-25 micrometers and transferring to a 1.5ml microcentrifuge tube (Eppendorf, Hamburg, Germany). Spores were concentrated by centrifugation at 900xG for 10 minutes (min). The supernatant was discarded, and spore pellets were combined and resuspended in 1ml autoclaved Arrowhead® bottled spring water (Nestle, Vevey, Switzerland). Spore concentration was calculated by counting

viable spores (non-germinated asexual spores that illuminated under phase optics with a light microscope) using a Neubauer Improved C-Chip Hemocytometer® (SKC Inc., Covington, GA, USA).

Experiment Preparation and Daily Maintenance

Aedes aegypti eggs, derived from the USDA-ARS Gainesville line, were purchased (Benzon Research Inc., Carlisle, PA, USA) and stored at room temperature for 7 days. Histology containers (Fisher Scientific, Pittsburgh, PA, USA) containing 350ml of bottled spring water were autoclaved. Four containers were assigned to each of four experimental treatments A, B, C, D (non-fungal larvae, fungal larvae, non-fungal adults, fungal adults, respectively). Approximately 50 eggs were added to each rearing container, which were covered with 4 layers of autoclaved Miracloth to mitigate airborne contamination, and were separately placed in a vacuum chamber (SP Industries Inc., Warminster, PA, USA) for 30 min to synchronize egg hatch timing (as described in Foggie and Achee, 2009). The larval mosquito food source was prepared by finely grinding Tetramin Fish Food (Tetra, Melle, Germany) with a mortar and pestle and suspending 0.2 grams (g) of fish food powder in 10ml of autoclaved bottled spring water. One milliliter of this slurry was added to each rearing container at the start of the experiment. Rearing containers from treatments B and D were inoculated with approximately 400,000 fungal trichospores. All mosquitoes were reared at 24°C +/- 1°C with a 16:8 hour light/dark cycle in a low temperature refrigerated incubator (Fisher Scientific, model #3724). Rearing containers were removed from the incubator daily, counts of the mosquitoes and their estimated larval instar stages recorded, and 1-2ml of

fish slurry added. All maintenance protocols were performed on a sterilized laboratory workbench next to a Bunsen burner to minimize contamination.

Larval Digestive Tract Visualization

Third and fourth instar larvae were collected from all treatments with at least one collected for 14 of the 16 experimental replicates to visualize fungal infestation in treatments B and D and to check for fungal contamination in treatments A and C. Eight dissections were performed on larvae from treatment A, 14 from treatment B, 9 from treatment C, and 15 from treatment D. Hindguts were removed and visualized with phase-contrast and Nomarski microscopy to observe and record fungal infestation rates in the digestive tracts of experimental larvae (Table B.1). No fungal material was recorded in treatments A or C.

Mosquito Sample Collection

Fourth instar larvae from treatments A and B were individually transferred to sterile 1.5ml microcentrifuge tubes and surface-sterilized using a modified larval protocol described in Coon et al., 2014. Microbial DNA extractions were performed on larvae after surface-sterilization. Mosquitoes from treatments C and D were reared to the pupae, transferred to sterile 1.5ml microcentrifuge tubes, and surface-sterilized following a modified adult protocol described in Coon et al., 2014. Surface-sterilized pupae were transferred separately to sterile 15ml centrifuge tubes (Corning Inc., Corning, NY, USA) containing 7ml autoclaved bottled spring water and reared axenically for 2-3 days until adult emergence. The sex of newly emerged adults was visually identified, individual adults were transferred to sterile 1.5ml microcentrifuge tubes, and microbial DNA extractions were performed on female mosquitoes.

Microbial DNA Extraction

Microbial DNA was extracted from larvae, adults, and other possible experimental sources with the Quick-DNA Fungal/Bacterial Kit® (Zymo Research, Irvine, CA, USA) following the protocol provided by the manufacturer with the following modifications: Lysis buffer was added directly to the 1.5ml microcentrifuge tubes containing harvested mosquitoes. Mosquitoes were manually ruptured in the microcentrifuge tubes with an autoclaved pellet pestle (DWK Life Sciences, Wertheim, Germany) for approximately 30 seconds (s) for larvae and 1-2 min for adults. Homogenized tube mixtures were transferred to bead tubes supplied with the extraction kit and were disrupted using a vortex mixer at maximum setting for 5 min. The elution buffer was heated to 45°C prior to its application to the spin-filters supplied by the extraction kit and remained on the filter surface for 5 min prior to the final elution spin. Extracted microbial DNA was stored at -80°C.

At least 4 DNA extractions were performed on mosquitoes from each replicate container for non-fungal larvae, non-fungal adults, and fungal adults, and at least 2 DNA extractions were performed from each replicate container for fungal larvae. Other DNA extractions were carried out on approximately 400,000 *Z. culisetae* trichospores, 50 *A. aegypti* eggs, and fish food slurry over the course of 3 days after original preparation. Additional DNA extractions were performed on a suite of negative control samples. These included extractions of autoclaved spring water, blank extraction kit reagents from the 4 kits used, rearing water from an empty rearing container across 3 experimental time points, and autoclaved water from two 15ml centrifuge tubes containing surface-sterilized pupae. Two blank PCR were also carried out to identify potential contamination of PCR

reagents. All PCR reactions were performed using 5PRIME HotMasterMix (Quantabio, Beverly, MA, USA).

Amplification of Fungal 18S rDNA

Targeted 18S rDNA PCR using primer pair TR3/TR4 (Tables B.2, 3, 4: Rxn_1) were performed on DNA extracted from 18 surface-sterilized larvae collected from treatment B for confirmatory detection of *Z. culisetae* (Rizzo and Pang, 2005). PCR products were visualized on 1.5% agarose gels and 17 of the 18 samples successfully amplified. All 18 samples were selected for sequencing.

Amplification of Bacterial 16S rDNA

The V3/V4 hypervariable regions of the microbial 16S rDNA gene were amplified with primer pair 341f/785r (Klindworth et al., 2013), with linker sequences (Takahashi et al., 2014), and adapter and spacer sequences provided by the University of Idaho GRC (University of Idaho, Moscow, ID, USA) (Table B.2: Rxn_2). Targeted 16S PCR were carried out (Tables B.3, 4: Rxn_2) on extracted experimental DNA samples with four 341f/785r primer pair variants containing spacer sequences of different lengths to mitigate amplification biases. PCR products were visualized on 1.5% agarose gels to confirm amplification of 16S rDNA. Additional targeted 16S PCR were carried out (Tables B.2, 3, 4: Rxn_3) on a subset of experimental samples spiked with DNA extracted from the halophilic bacterium, *Salinibacter ruber* (ATCC product BAA-605D-5). *Salinibacter ruber* DNA concentration was quantified with a Qubit Fluorometer® (Invitrogen, Carlsbad, CA, USA) and 16S copies per nanogram of DNA were calculated. Approximately 1,000,000 16S copies were added in addition to experimental sample template DNA for use in SCML analyses (Stämmler et al., 2016).

Preparation and Sequencing of 16S Amplicons

Secondary PCR were performed (Tables B.2, 3, 4: Rxn_4) to attach barcode sequences provided by the University of Idaho GRC to PCR amplicons. Amplicons were visualized on 1.5% agarose gels and pooled based on gel band intensity. Amplicon sequencing was performed with an Illumina MiSeq v3 (Illumina Inc., San Diego, CA, USA) at the University of Idaho GRC, which produced 300 base pair (bp) paired-end reads. Reads were demultiplexed by sample barcode sequences by the sequencing facility.

Raw Read Processing and OTU Assignment

Amplicon lengths were estimated using FLASH (Magoč and Salzberg, 2011) for a subset of samples. The majority of amplicons were estimated at 430bp or shorter (Figure A.1). Paired-end reads were processed using the DADA2 pipeline (Callahan et al., 2016). Forward and reverse reads were trimmed to 278bp and 167bp, respectively, trimmed at the location of the first occurrence of a base call with a Phred score less than or equal to 15, and were filtered by removing reads with any number of N base calls or containing greater than or equal to 6 estimated errors. Reads were merged with a minimum overlap of 12 bases. Experimental samples with less than 100 reads after initial filtering were removed from the pipeline. Chimeric sequences were discarded, and merged reads were dereplicated and clustered into OTUs based on 97% sequence similarity. Read counts were calculated and tracked for each step in the workflow (Table B.5). Taxonomy was assigned to OTUs using the SILVA v132 database (Pruess et al., 2007; Quast et al., 2013). A neighbor-joining tree was inferred using the *phangorn* package in R (Schliep, 2011) and a generalized time-reversible with gamma rate variation maximum likelihood

tree was fit using the neighbor-joining tree as the starting point. The phylogenetic tree, taxonomically assigned OTUs, read count data, and experimental sample metadata were combined into a single object using the *Phyloseq* package in R (McMurdie and Holmes, 2013).

Phyloseq Object Data Preparation and Analyses

Of the negative controls sequenced, 3 of the 4 extraction kits had over 100 reads after initial filtering and chimeric sequence removal in the DADA2 pipeline, while all other negative controls sequenced had less than 100 reads and were removed from analyses (Table B.5). Reagents from extraction kits add contaminant sequences to experimental samples (Salter et al., 2014) and the removal of contaminant OTUs is recommended to ensure the quality and accuracy of sequencing data analyses. Contaminant sequences introduced from all 4 kits combined were identified with the *decontam* package in R (Davis et al., 2018) using the "prevalence" method and the threshold set to 0.5. All OTUs identified as kit contaminants were removed prior to downstream analyses.

Data from the Phyloseq object were subset into unique datasets and independently processed for comparative analyses for larva type (non-fungal and fungal), adult type (non-fungal and fungal), developmental stage of non-fungal mosquitoes (larvae and adults) and fungal mosquitoes (larvae and adults), and a set of positive controls (food and eggs). Alpha diversity measures of Simpson and Shannon diversity indices were calculated using the estimate_richness function in *Phyloseq*, and boxplots were generated in *ggplot2* (Wickham, 2011). CV values (the ratio of the standard deviation to the mean) have been used as a metric to measure variation in alpha diversity across groups (Flores

et al., 2014; Galloway-Peña et al., 2017). Coefficient of variation values for each alpha diversity metric in each group compared were calculated with the cv function in the *sjstats* package in R (Lüdecke, 2018). The R package *cvequality* (Marwick and Krishnamoorthy, 2018) was used to test for significant differences of CV values for alpha diversity measures using an asymptotic test (Feltz and Miller, 1996) and a MSLRT (Krishnamoorthy and Lee, 2014).

Rarefaction curves were generated using the ggrare function in the *ranacapa* package (Kandlikar et al., 2018) along with *ggplot2* in R (Figure A.2). Rarefaction read cutoff values were selected for each dataset independently to maximize richness captured while minimizing the number of samples cut for each comparative analysis (Table B.5). Singletons were removed and datasets were further processed by discarding OTUs that were not represented by at least 6 reads in one sample within a dataset after rarefaction.

Beta diversity measures of Bray-Curtis dissimilarity, unweighted UniFrac, and weighted UniFrac distances were calculated in *Phyloseq*, and tests for significant differences due to the main effect in a comparison (Treatment or Developmental Stage) were carried out with PERMANOVA (Anderson, 2017) with 999 permutations using the adonis function in the *Vegan* package in R (Dixon, 2003) in combination with the nested.npmanova function in the *BiodiversityR* package in R (Kindt, 2016). Nested PERMANOVA calculated the correct pseudo-F and *P* values for the main effect and accounted for random effects across rearing containers. Dispersions of beta diversity measures can be calculated and utilized as an additional comparative metric (Anderson et al., 2006). Variances of beta diversity measures for each group were calculated using the betadisp function in *Vegan*. Permutational statistical tests for the homogeneity of

dispersions in each group comparison (Anderson, 2006) were calculated with the permute.test function in *Vegan* with 999 permutations. Boxplots of the dispersals were created in *ggplot2*, and NMDS plots of beta diversity measures were created using the plot_ordination function in *Phyloseq* along with *ggplot2*. Relative abundances of the top 15 bacterial families shared between groups (which accounted for greater than 80% of the total reads) in each dataset were calculated, and stacked bar plots were created using the plot_bar function in *Phyloseq* in combination with *ggplot2*.

SCML Read Processing

Combined data from the Phyloseq object were subset for samples that were spiked with *S. ruber* DNA. A conversion factor was calculated by dividing the number of *S. ruber* reads in each sample by the average number of *S. ruber* reads in a group. Total read counts for each sample were calibrated by multiplying the total reads by the sample-specific conversion factor so that all samples had the same read counts for *S. ruber*.

Linear Mixed Models

The statistical significance of the main effect on mean alpha diversity measures, relative abundances of each of the top 15 bacterial families shared between groups, and the SCML calibrated read counts for each dataset were calculated by fitting a linear mixed model to account for random effects across rearing containers using the lmer function in the *lme4* package in R (Bates et al., 2015). Models were tested with Type II Wald F tests with Kenward-Roger degrees of freedom using the Anova function in the *car* package in R (Fox et al., 2018).

Results

Fungal Infestation Reduces Microbiome Taxonomic Composition Variation in Larvae

Reads for non-fungal and fungal larvae were rarefied to 5251 reads, with 154 OTUs identified across 38 samples. Linear mixed models did not detect a significant difference in mean alpha diversity measures due to fungal infestation (Table B.6). PERMANOVA did not detect a fungal infestation effect on beta diversity measures (Table B.7), however, unweighted UniFrac distance dispersal was higher in non-fungal larvae ($F_{(1, 36)}$= 4.6534, P=0.036, Figure 2.E). Relative abundances of the top 15 bacterial families shared between non-fungal and fungal larvae were calculated and plotted (Figure 3.A). Linear mixed models did not detect differences in relative abundances due to fungal infestation (Table B.8).

Fungal Infestation Reduces Transstadial Transmission Pattern Variation and Affects Transference of Certain Taxa

Reads for non-fungal larvae and adults were rarefied to 2560 reads, with 484 OTUs identified across 36 samples. Linear mixed models did not detect differences in mean alpha diversity measures across developmental stages (Table B.6), however, CV values were higher in adults for Simpson (P<0.001, Figure 1.A) and Shannon (P<0.001, Figure 1.B) diversity indices. PERMANOVA detected differences in Bray-Curtis dissimilarity (Pseudo-$F_{(1, 6)}$=3.7052, P=0.022), unweighted UniFrac (Pseudo-$F_{(1, 6)}$=6.9677, P=0.035), and weighted UniFrac distances (Pseudo-$F_{(1, 6)}$=8.9194, P=0.031) across developmental stages (Table B.7). Non-metric multidimensional scaling plots show separation between larvae and adults for these metrics (Figure 2.A, B, C). Beta diversity variation was higher in adults relative to larvae for Bray-Curtis dissimilarity

($F_{(1, 34)}$=31.461, P<0.001, Figure 2.D) and unweighted UniFrac distance ($F_{(1, 34)}$=43.821, P<0.001, Figure 2.E). Relative abundances of the top 15 bacterial families shared between non-fungal larvae and adults were calculated and plotted (Figure 3.B). Linear mixed models detected differences in relative abundances for certain families across developmental stages (Table B.8). *Microbacteriaceae* and *Rhizobiaceae* decreased in adults relative to larvae (P=0.002, P=0.015, respectively), whereas *Burkholderiaceae* increased (P=0.002).

Reads for fungal larvae and adults were rarefied to 2229 reads, with 600 OTUs identified across 31 samples. Linear mixed models detected differences in mean alpha diversity measures across developmental stages for Shannon Diversity (P=0.011, Figure 1.B) (Table B.6). Coefficient of variation values were not different for Simpson or Shannon diversity indices (Table B.6). PERMANOVA detected differences in beta diversity for Bray-Curtis dissimilarity (Pseudo-$F_{(1,6)}$=6.2994, P=0.028), unweighted UniFrac (Pseudo-$F_{(1,6)}$=10.7434, P=0.03), and weighted UniFrac distances (Pseudo-$F_{(1,6)}$=8.4334, P=0.025) across developmental stages (Table B.7). Non-metric multidimensional scaling plots show separation between larvae and adults for these metrics (Figure 2.A, B, C). Beta diversity variation was higher in adults relative to larvae for Bray-Curtis dissimilarity ($F_{(1, 29)}$=32.067, P<0.001, Figure 2.D) and unweighted UniFrac distance ($F_{(1, 29)}$=53.22, P<0.001, Figure 2.E). Relative abundances of the top 15 bacterial families shared between fungal larvae and adults were calculated and plotted (Figure 3.C). Linear mixed models detected differences in relative abundances for certain families across developmental stages (Table B.8). *Microbacteriaceae* and *Rhizobiaceae*

decreased in adults relative to larvae (P=0.013, P=0.013, respectively), whereas *Corynebacteriaceae* increased (P=0.002).

Altered Transstadial Transmission Patterns Lead to Distinct Microbiomes in Newly Emerged Adults

Reads for non-fungal and fungal adults were rarefied to 1777 reads, with 881 OTUs identified across 33 samples. Linear mixed models did not detect differences in mean alpha diversity measures due to fungal infestation during the larval stage (Table B.6), however, CV values were higher in non-fungal adults for Simpson ($P < 0.001$, Figure 1.A) and Shannon ($P < 0.001$, Figure 1.B) diversity indices. PERMANOVA did not detect a larval fungal infestation effect for Bray-Curtis dissimilarity or unweighted UniFrac distance (Table B.7), though weighted UniFrac distance had a low P value (Pseudo-$F_{(1, 6)}$=5.6849, P=0.05). Relative abundances of the top 15 bacterial families shared between non-fungal and fungal adults were calculated and plotted (Figure 3.D). Linear mixed models detected differences in relative abundances of certain taxa due to larval fungal infestation (Table B.8). *Corynebacteriaceae* and *Moraxellaceae* had higher relative abundance in fungal relative to non-fungal adults (P=0.025, P=0.048, respectively).

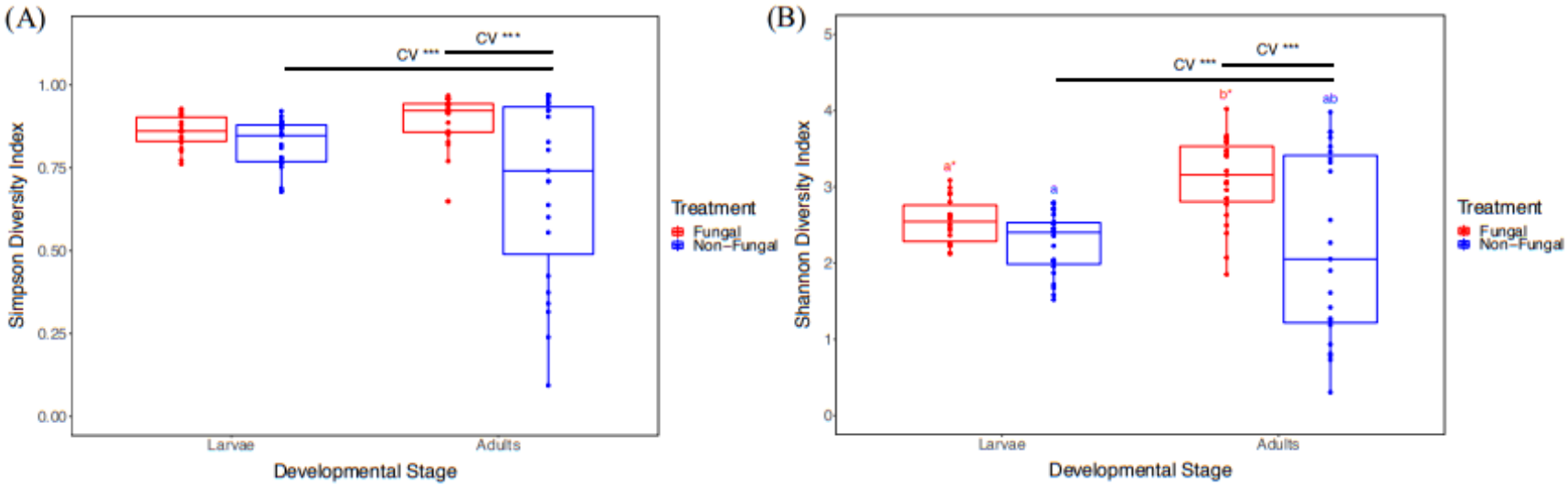

Figure 1. Boxplots of Alpha Diversity Measures

Boxplots of alpha diversity measures for Simpson (A) and Shannon (B) diversity indices of microbiome communities in fungal (red) and non-fungal (Blue) mosquitoes collected at larval and adult stages. Solid lines in each boxplot represent median values and horizontal edges of the boxes indicate quartiles. Statistical results from linear mixed models comparing mean alpha diversity measures between treatments and across developmental stages within treatments are indicated with lowercase letters above each boxplot, with significant results indicated with asterisks. Significant combined results of asymptotic and MSLRT comparing CV values between treatments and across developmental stages within treatments are indicated with solid black lines labeled “CV” above boxplots. Statistical significance of comparative analyses is indicated with *$p<0.001$.

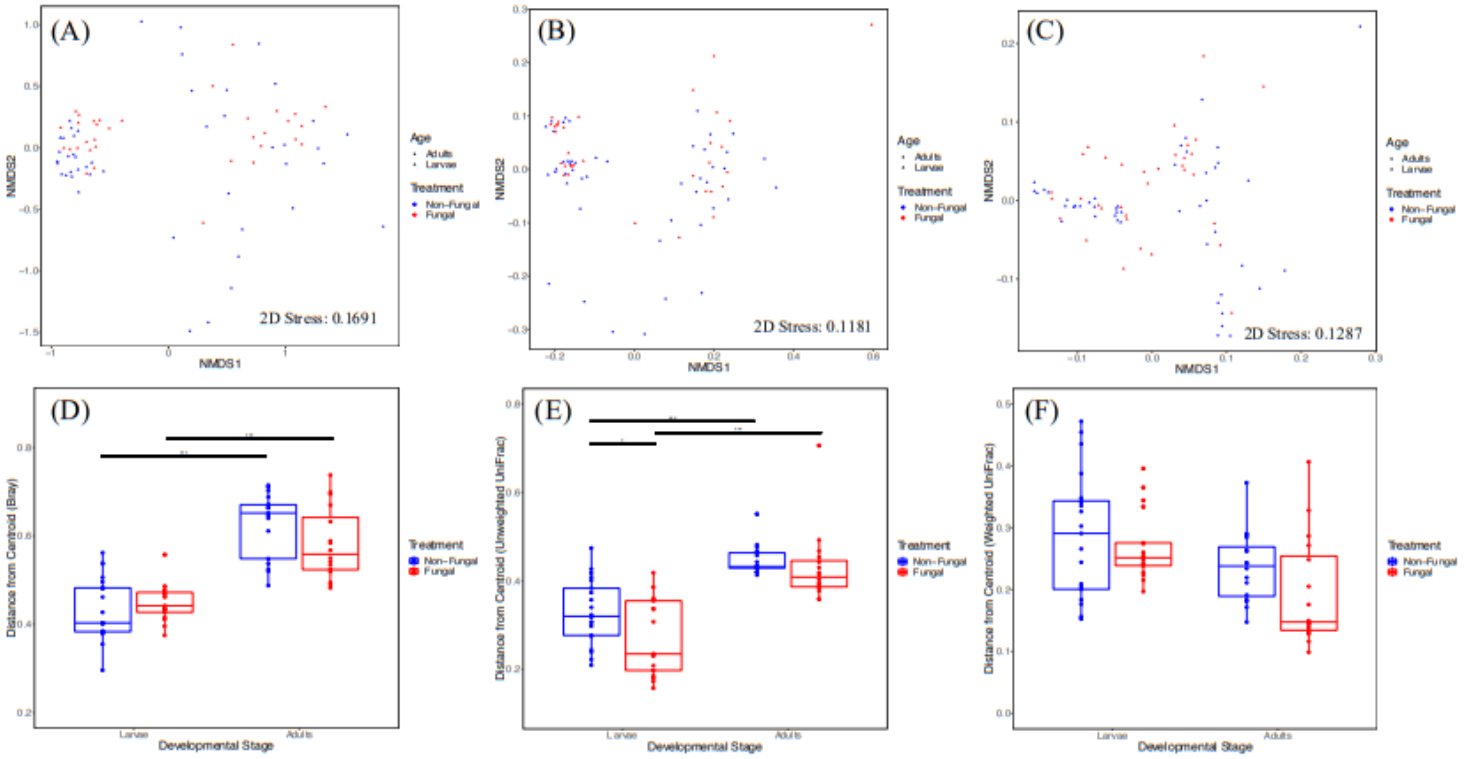

Figure 2. NMDS Plots of Beta Diversity Measures and Boxplots of Group Dispersals

Beta diversity measures visualized with NMDS plots for Bray Curtis dissimilarity (- A), unweighted UniFrac (B), and weighted UniFrac (C) distances for mosquito microbiomes between fungal (red) and non-fungal (blue) treatments and across developmental stages within treatments. Boxplots representing beta diversity variance for each group are shown for Bray Curtis dissimilarity (D), unweighted UniFrac (E), and weighted UniFrac (F) measures. Solid lines in each boxplot represent median values and horizontal edges of the boxes indicate quartiles. Variance of measures for each group were calculated by measuring the distance of each sample to the group centroid for each metric. Significant results from comparisons of mean beta diversity variance using permutational tests for homogeneity of dispersals are indicated by solid black lines above boxplots. Statistical significance of comparative analyses is indicated with *P<0.05, **P<0.01, ***P<0.001

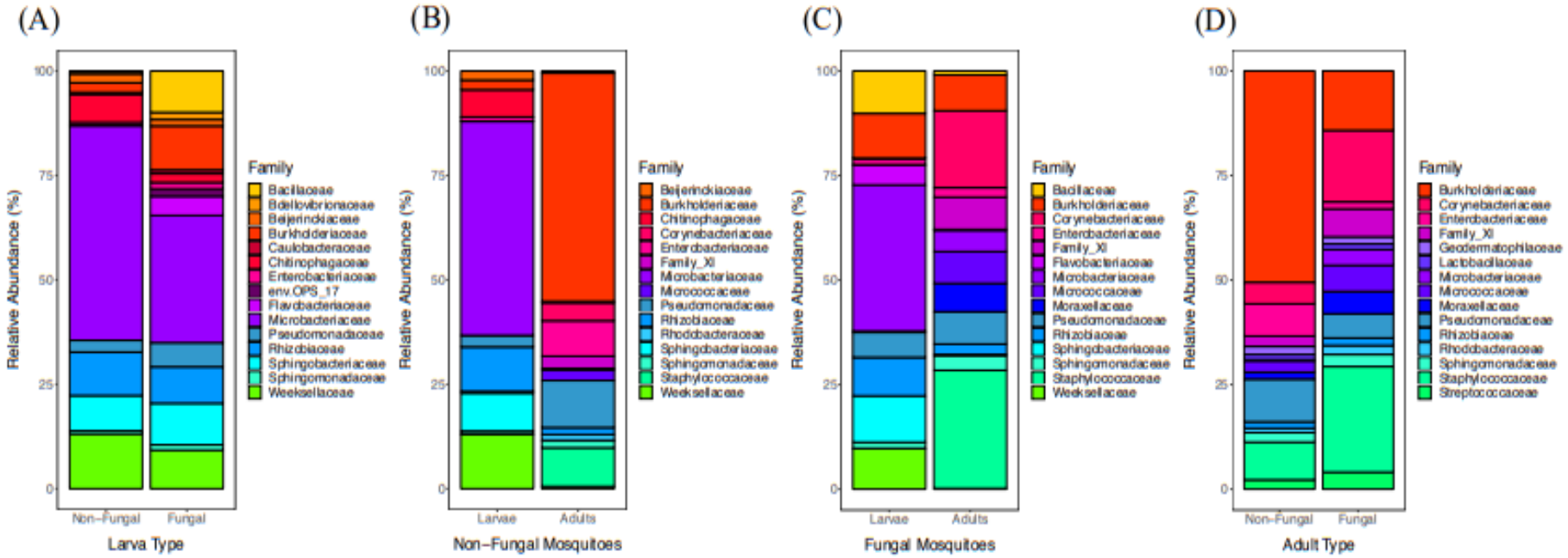

Figure 3. Bar Plots of the Relative Abundances of the Top 15 Bacterial Families Shared within each Dataset

Relative abundances of the top 15 bacterial families shared between non-fungal and fungal larvae (A), non-fungal larvae and adults (B), fungal larvae and adults (C), and newly emerged non-fungal and fungal adults (D). Colored segments in each bar represent different bacterial families and the height of each segment corresponds to the relative percentage of reads assigned to a given family out of the total reads belonging to the top 15 families shared between groups. Family colors are consistent across all plots.

Larval Microbiomes Have Larger Bacterial Loads than Adults

Total reads for 16 non-fungal and 26 fungal larvae and adults were calibrated using the SCML method. Linear mixed models showed that larvae had higher calibrated read counts than adults for both groups (P=0.019, P=0.038, respectively) (Figure A.3, Table B.9).

Discussion

Laboratory-based experiments with *A. aegypti* revealed distinct microbial transstadial transmission patterns and taxonomic compositions in mosquitoes infested with *Z. culisestae*. In non-fungal mosquitoes, no differences in mean alpha diversity measures were detected, however, CV values were higher in adults relative to larvae for Simpson (P<0.001, Figure 1.A) and Shannon diversity (P<0.001, Figure 1.B) indices (Table B.6), indicating that newly emerged non-fungal adult microbiomes have higher variability in taxonomic diversity and distribution than larvae. In contrast, mean alpha diversity measures in fungal mosquitoes were higher in adults relative to larvae for Shannon diversity (P=0.011, Figure 1.B). Additionally, no differences in CV values were detected for Simpson (P<0.14) or Shannon diversity (P<0.1) indices (Table B.6), demonstrating that fungal infestation of the larval digestive tract leads to higher taxonomic diversity, but similar distribution in newly emerged adult microbiomes relative to larvae.

For both groups of mosquitoes, beta diversity analyses showed divergent microbiomes between larvae and adults. In non-fungal mosquitoes, beta diversity differences for Bray-Curtis dissimilarity (P=0.022, Figure 2.A) and weighted UniFrac distance (P=0.031, Figure 2.C) showed clear shifts in microbiome compositional

structures, whereas the difference in unweighted UniFrac distance (P=0.035, Figure 2.B) indicated disparities in the microbial taxa present across developmental stages. These findings were conserved in fungal mosquitoes, where differences in beta diversity across developmental stages were detected for Bray-Curtis dissimilarity (P=0.028, Figure 2.A), unweighted UniFrac (P=0.03, Figure 2.B), and weighted UniFrac distances (P=0.025, Figure 2.C). Additionally, beta diversity variation was higher in adults relative to larvae for both non-fungal and fungal mosquitoes for Bray-Curtis dissimilarity (P<0.001, Figure 2.D) and unweighted UniFrac distance (P<0.001, Figure 2.E), demonstrating that the mosquito microbiome undergoes changes in compositional structure across developmental stages, supporting findings from (Wang et al., 2011; Gimonneau et al., 2014; Duguma et al., 2015), regardless of fungal infestation. Additionally, these data show that newly emerged adults harbor microbiomes with higher variability in taxonomic composition and structure relative to larvae.

Whereas statistical analyses showed significant changes in microbiomes across developmental stages, certain bacterial families present in larvae were observed in newly emerged adults (Table B.8). Shifts in relative abundances of certain taxa in adults relative to larvae were observed in both non-fungal (Figure 3.B) and fungal (Figure 3.C) mosquitoes. These observations support other studies that revealed adults inherit a subset of their associated microbiota from larvae and pupae through transstadial transmission (Wang et al., 2011; Coon et al., 2014; Chen et al., 2015; Duguma et al., 2015). Fungal infestation affects the outcomes of transstadial transmission for certain taxa. In non-fungal mosquitoes, *Burkholderiaceae*, a minor community member in larvae (2.23%), was transferred to adults and became the dominant taxon (42.16%, P=0.002). In contrast,

Burkholderiaceae in fungal larvae (9.57%) did not increase in adults (5.59%, *P*=0.511), demonstrating that fungal infestation leads to differential transstadial transmission of certain taxa. Conversely, in both groups of mosquitoes *Microbacteriaceae* was the dominant taxon in larval microbiomes (49.47% in non-fungal, 31.26% in fungal), as was recorded in Coon et al., 2014, and decreased to low abundances in adults (0.30%, *P*=0.002, non-fungal; 3.32%, *P*=0.013, fungal). A similar pattern was observed for *Rhizobiaceae*, which was present at moderate levels in larvae from both groups (10.26% in non-fungal, 8.23% in fungal), but decreased to low abundances in adults (1.28%, *P*=0.015, non-fungal; 1.61%, *P*=0.013, fungal). Collectively, these data demonstrate that only certain bacterial taxa are capable of successful transstadial transmission, and fungal infestation can lead to differential relative abundances of these taxa in newly emerged adults.

Direct comparisons between non-fungal and fungal adults revealed that the transstadial transmission patterns impacted the compositions and structures of microbiomes in newly emerged adults. Whereas no difference was detected for mean alpha diversity measures, fungal adults had high values for alpha diversity indices and lower CV values for Simpson (*P*<0.001, Figure 1.A) and Shannon diversity (*P*<0.001, Figure 1.B) than non-fungal adults, indicating that fungal mosquitoes emerged with distinct microbiomes characterized by high richness and even taxonomic distribution. In contrast, non-fungal adults had high CV values for alpha diversity measures and emerged with variable microbiome compositional structures. Many of the non-fungal adults had low values for Shannon and Simpson diversity indices, indicative of microbiomes with low diversity and high levels of dominance by certain taxa. The wide dispersal of these

measures could be a reflection of variable *Burkholderiaceae* dominance in non-fungal adult microbiomes. This family only increased in non-fungal adults, though it was present on mosquito eggs (Figure A.4) and both mosquito groups would have been exposed to it.

Altered transstadial transmission patterns resulted in distinct adult microbiome taxonomic compositions. The family *Corynebacteriaceae*, had higher relative abundance in fungal (12.58%) relative to non-fungal (4.08%) adults (P=0.025). This taxon was present in the fish slurry fed to all mosquitoes during the experiment (Figure A.4). Additionally, *Moraxellaceae* was also higher in fungal (3.91%) relative to non-fungal (1.31%) adults (P=0.048), and was found on the mosquito eggs (Figure A.4). The disparity in the relative abundances of these families in newly emerged adults demonstrates differential establishment of certain bacterial taxa, possibly a result of altered microbiome dynamics influenced by larval fungal infestation. There is evidence of variable taxonomic composition in non-fungal larvae based on the high dispersal of unweighted UniFrac distance (P=0.036, Figure 2.E). In the absence of fungal infestation, certain taxa may differentially proliferate in larvae, leading to variable transstadial transmission patterns often resulting in adult microbiomes with low taxonomic diversity and high levels of dominance by *Burkholderiaceae*. In contrast, fungal infestation could reduce taxonomic composition variability in larvae, resulting in highly diverse adult microbiomes with low levels of dominance by *Burkholderiaceae*. Suppression of *Burkholderiaceae* establishment in fungal adults by fungal-bacterial-host interactions in larvae may have provided opportunities for other taxa to establish during or after pupation. This hypothesis is supported by the consistently high measures for Simpson and Shannon diversity indices in fungal adults.

SCML analyses (Stämmler et al., 2016) revealed that newly emerged adults harbor microbiomes with smaller bacterial loads relative to larvae for both non-fungal and fungal mosquitoes (Figure A.3, Table B.9). Small adult bacterial loads may be due to the conserved reduction of *Microbacteriaceae* and *Rhizobiaceae* in adults. If these taxa inhabit the digestive tract in larvae, this decrease could be the result of morphological and physiological processes that occur during and after pupation (Moll et al., 2011 and Moncayo et al., 2005). However, certain taxa are successfully transstadially transmitted in both groups of mosquitoes and increase in relative abundance in adults. It is unclear whether these bacteria were established in the digestive tract or other anatomical regions in the larvae. These taxa may inhabit larval salivary glands (Sharma et al., 2014), hemocoels (Brown et al., 2018), or malpighian tubules (Chavshin et al., 2013; Chavshin et al., 2015), allowing for successful transmission across developmental stages. Furthermore, it is unknown whether these taxa subsequently colonized the newly emerged adult digestive tract, as was observed in Chavshin et al., 2013 and Chavshin et al., 2015. Implementation of fluorescence-based-assays on identified transstadially transmitted taxa would allow for the investigation of these transmission pathways. This could also reveal potential spatial interactions that occur between fungi and bacteria, which could help explain the differential transstadial transmission patterns and adult microbiome compositions recorded in this experiment. Other studies should investigate the role that dominant bacterial taxa, such as *Burkholderiaceae* and *Microbacteriaceae*, have on influencing transmission and establishment dynamics of other microbial community members during and after pupation by utilizing inoculation experiments of gnotobiotic larvae similar to studies previously described in Coon et al., 2014 and

Dickson et al., 2017. Understanding the morphological and physiological mechanisms occurring in the mosquito holobiont that affect transstadial transmission of bacteria is crucial to reveal the interactions involved in the formation of microbiomes in newly emerged adults, which may impact host vector competence. Future research could investigate these processes by utilizing fungal infestation protocols used in this experiment along with vector competence assays (see Gonçalves et al., 2014 and Dickson et al., 2017). If fungal infestation influences these interactions, it is possible that microbial communities associated with mosquito populations that exhibit variable vector competence (Charan et al., 2013 and Gonçalves et al., 2014) are impacted by fungal-bacterial-host interactions.

Perspectives

The microbial communities analyzed in this study represent snapshots of the newly emerged adult microbiome formed by transstadial transmission in a laboratory environment. However, adult microbiomes are influenced by nutrient intake (Rani et al., 2009; Oliveira et al., 2011; Wang et al., 2011; Terenius et al., 2012) and shift in composition and structure during adult development (Muturi et al., 2016a). Future research should analyze whether the altered transstadial transmission patterns observed in this experiment influence the formation of the adult microbiome throughout its lifespan. This would help inform whether the patterns observed herein have long-lasting implications for mosquito-pathogen interactions and carryover impacts on human health issues. It should be noted that those results, and the results of other microbiome laboratory experiments, are not necessarily representative of microbiome dynamics in wild mosquito populations. Additionally, bacterial taxa have differential 16S gene copies

per genome. Relative abundances reported here may not accurately reflect absolute abundances of bacterial families.

The findings of this study may have been affected by several factors. Illumina sequencing yielded variable read coverage within and across the datasets analyzed. Rarefaction was used to minimize potential biases in taxonomic richness estimates, however, this may have led to underestimations of microbial diversity. Additionally, efforts were made to limit bacterial exposure of experimental mosquitoes to egg microbes and those in the fish slurry (Figure A.4). Although protocols were implemented to mitigate external laboratory contamination, some levels of contamination may have affected results (Salter et al., 2014). Negative control samples were sequenced to account for this, and the *decontam* package in R was used to identify and remove contaminant OTU sequences found in extraction kit reagents. As with all microbiome studies, independent replication under different laboratory conditions will be essential to confirm the findings of this and other such experiments, as has been proposed and implemented in human microbiome studies (Sinha et al., 2015; Sinha et al., 2017). Finally, fungal infestation could not be directly quantified for DNA extracted from fungal larvae. Targeted 18S PCR were performed to confirm the presence of fungal DNA at larval harvest, though it is likely that larvae collected from this treatment had varying levels of fungal infestation, possibly influencing our results and conclusions.

Conclusion

Fungal interactions in host microbiomes are often overlooked. Our results provide the first evidence that mosquito larvae infested with an endosymbiotic gut fungus experience distinct fungal-bacterial-host interactions that reduce transstadial transmission

variability and result in microbiomes characterized by high taxonomic diversity, even distributions, and unique compositions. These results emphasize that future microbiome studies include fungal data in analyses of microbe-host interactions. Mosquitoes have significant impacts on human health worldwide, and the study of biotic interactions that affect their fitness is essential to fully understand the factors driving mosquito vector competence for human pathogens. We hope that the findings from this experiment will encourage future collaboration between microbial ecologists and mycologists to improve the scientific community's ability to holistically and accurately analyze host-microbe systems.

REFERENCES

Alencar YB, Ríos-Velásquez CM, Lichtwardt RW, Hamada N. Trichomycetes (Zygomycota) in the Digestive Tract of Arthropods in Amazonas, Brazil. *Mem Inst Oswaldo Cruz* 2003; **98**: 799–810.

Anderson MJ. Distance-based tests for homogeneity of multivariate dispersions. *Biometrics* 2006; **62**: 245–253.

Anderson MJ, Ellingsen KE, McArdle BH. Multivariate dispersion as a measure of beta diversity. *Ecol Lett* 2006; **9**: 683–693.

Anderson MJ. Permutational Multivariate Analysis of Variance (PERMANOVA). *Wiley StatsRef: Statistics Reference Online* 2017; 1–15.

Angleró-Rodríguez YI, Talyuli OAC, Blumberg BJ, Kang S, Demby C, Shields A, et al. An *Aedes aegypti*-associated fungus increases susceptibility to dengue virus by modulating gut trypsin activity. *Elife* 2017; **6**: e28844.

Apte-Deshpande A, Paingankar M, Gokhale MD, Deobagkar DN. *Serratia odorifera* a midgut inhabitant of *Aedes aegypti* mosquito enhances its susceptibility to dengue-2 virus. *PLoS One* 2012; **7**: e40401.

Audsley MD, Seleznev A, Joubert DA, Woolfit M, O'Neill SL, McGraw EA. *Wolbachia* infection alters the relative abundance of resident bacteria in adult *Aedes aegypti* mosquitoes, but not larvae. *Mol Ecol* 2018; **27**: 297–309.

Bates D, Maechler M, Bolker B, Walker S, Maechler Martin, Walker S. Package 'lme4': Linear Mixed-Effects Models using 'Eigen' and S4. *J Stat Softw* 2015.

Bian G, Xu Y, Lu P, Xie Y, Xi Z. The Endosymbiotic Bacterium *Wolbachia* Induces Resistance to Dengue Virus in *Aedes aegypti*. *PLoS Pathog* 2010; **6**: e1000833.

Bourtzis K, Dobson SL, Xi Z, Rasgon JL, Calvitti M, Moreira LA, et al. Harnessing mosquito-*Wolbachia* symbiosis for vector and disease control. *Acta Trop* 2014; **132**: S150–S163.

Brown LD, Thompson GA, Hillyer JF. Transstadial transmission of larval hemocoelic infection negatively affects development and adult female longevity in the mosquito *Anopheles gambiae*. *J Invertebr Pathol* 2018; **151**: 21–31.

Callahan BJ, McMurdie PJ, Rosen MJ, Han AW, Johnson AJA, Holmes SP. DADA2: High-resolution sample inference from Illumina amplicon data. *Nat Methods* 2016; **13**: 581–583.

Carissimo G, Pondeville E, McFarlane M, Dietrich I, Mitri C, Bischoff E, et al. Antiviral immunity of *Anopheles gambiae* is highly compartmentalized, with distinct roles for RNA interference and gut microbiota. *Proc Natl Acad Sci* 2015; **112**: E176–E185.

Chandler JA, Liu RM, Bennett SN. RNA Shotgun Metagenomic Sequencing of Northern California (USA) Mosquitoes Uncovers Viruses, Bacteria, and Fungi. *Front Microbiol* 2015; **6**: 1–16.

Charan SS, Pawar KD, Severson DW, Patole MS, Shouche YS. Comparative analysis of midgut bacterial communities of *Aedes aegypti* mosquito strains varying in vector competence to dengue virus. *Parasitol Res* 2013; **112**: 2627–2637.

Chavshin AR, Oshaghi MA, Vatandoost H, Yakhchali B, Raeisi A, Zarenejad F. *Escherichia coli* expressing a green fluorescent protein (GFP) in *Anopheles stephensi*: A preliminary model for paratransgenesis. *Symbiosis* 2013; **60**: 17–24.

Chavshin AR, Oshaghi MA, Vatandoost H, Yakhchali B, Zarenejad F, Terenius O. Malpighian tubules are important determinants of *Pseudomonas* transstadial transmission and longtime persistence in *Anopheles stephensi*. *Parasites and Vectors* 2015; **8**: 36.

Chen S, Bagdasarian M, Walker ED. *Elizabethkingia anophelis*: Molecular manipulation and interactions with mosquito hosts. *Appl Environ Microbiol* 2015; **81**: 2233–2243.

Chouaia B, Rossi P, Epis S, Mosca M, Ricci I, Damiani C, et al. Delayed larval development in *Anopheles* mosquitoes deprived of *Asaia* bacterial symbionts. *BMC Microbiol* 2012; **12**: S2.

Coon KL, Vogel KJ, Brown MR, Strand MR. Mosquitoes rely on their gut microbiota for development. *Mol Ecol* 2014; **23**: 2727–2739.

Coon KL, Brown MR, Strand MR. Mosquitoes host communities of bacteria that are essential for development but vary greatly between local habitats. *Mol Ecol* 2016; **25**: 5806–5826.

Coon KL, Brown MR, Strand MR. Gut bacteria differentially affect egg production in the anautogenous mosquito *Aedes aegypti* and facultatively autogenous mosquito *Aedes atropalpus* (Diptera: Culicidae). *Parasites and Vectors* 2016; **9**: 375.

Davis NM, Proctor D, Holmes SP, Relman DA, Callahan BJ. Simple statistical identification and removal of contaminant sequences in marker-gene and metagenomics data. *Microbiome* 2018; **6**: 226.

Dennison NJ, Jupatanakul N, Dimopoulos G. The mosquito microbiota influences vector competence for human pathogens. *Curr Opin Insect Sci* 2014; **3**: 6–13.

Dickson LB, Jiolle D, Minard G, Moltini-Conclois I, Volant S, Ghozlane A, et al. Carryover effects of larval exposure to different environmental bacteria drive adult trait variation in a mosquito vector. *Sci Adv* 2017; **3**: e1700585.

Dickson LB, Ghozlane A, Volant S, Bouchier C, Ma L, Vega-Rúa A, et al. Diverse laboratory colonies of *Aedes aegypti* harbor the same adult midgut bacterial microbiome. *Parasites and Vectors* 2018; **11**: 207.

Dixon P. VEGAN, a package of R functions for community ecology. *J Veg Sci* 2003; **14**: 927–930

Dong Y, Manfredini F, Dimopoulos G. Implication of the mosquito midgut microbiota in the defense against malaria parasites. *PLoS Pathog* 2009; **5**: e1000423.

Duguma D, Rugman-Jones P, Kaufman MG, Hall MW, Neufeld JD, Stouthamer R, et al. Bacterial Communities Associated with *Culex* Mosquito Larvae and Two

Emergent Aquatic Plants of Bioremediation Importance. *PLoS One* 2013; **8**: e72522.

Duguma D, Hall MW, Rugman-Jones P, Stouthamer R, Terenius O, Neufeld JD, et al. Developmental succession of the microbiome of *Culex* mosquitoes Ecological and evolutionary microbiology. *BMC Microbiol* 2015; **15**: 140.

Feltz CJ, Miller GE. An asymptotic test for the equality of coefficients of variation from k populations. *Stat Med* 1996; **15**: 647–658.

Flores GE, Caporaso JG, Henley JB, Rideout JR a., Domogala D, Chase J, et al. Temporal variability is a personalized feature of the human microbiome. *Genome Biol* 2014; **15**: 531.

Foggie T, Achee N. Standard Operating Procedures : Rearing *Aedes aegypti* for the HITSS and Box Laboratory Assays Training Manual 2009; 1-18.

Fox J, Weisberg S, Price B, Adler D, Bates D, Baud-Bovy G. Package 'car'. *R Doc* 2018.

Gaio ADO, Gusmão DS, Santos A V., Berbert-Molina MA, Pimenta PFP, Lemos FJA. Contribution of midgut bacteria to blood digestion and egg production in *Aedes aegypti* (Diptera: Culicidae) (L.). *Parasites and Vectors* 2011; **4**: 105.

Galloway-Peña JR, Smith DP, Sahasrabhojane P, Wadsworth WD, Fellman BM, Ajami NJ, et al. Characterization of oral and gut microbiome temporal variability in hospitalized cancer patients. *Genome Med* 2017; **9**: 21.

Gimonneau G, Tchioffo M, Abate L, Boissiere A, Awono-Ambene P, Nsango S, et al. Composition of *Anopheles coluzzii* and *Anopheles gambiae* microbiota from larval to adult stages. *Infect Genet Evol* 2014; **28**: 715–724.

Gonçalves CM, Melo FF, Bezerra JMT, Chaves BA, Silva BM, Silva LD, et al. Distinct variation in vector competence among nine field populations of *Aedes aegypti* from a Brazilian dengue-endemic risk city. *Parasites and Vectors* 2014; **7**: 320.

Gusmão DS, Santos A V., Marini DC, Bacci M, Berbert-Molina MA, Lemos FJA. Culture-dependent and culture-independent characterization of microorganisms

associated with *Aedes aegypti* (Diptera: Culicidae) (L.) and dynamics of bacterial colonization in the midgut. *Acta Trop* 2010; **115**: 275–281.

Hegde S, Rasgon JL, Hughes GL. The microbiome modulates arbovirus transmission in mosquitoes. *Curr Opin Virol* 2015; **15**: 97–102.

Horn BW. Ultrastructural Changes in Trichospores of *Smittium culisetae* and *S. culicis* during in Vitro Sporangiospore Extrusion and Holdfast Formation. *Mycologia* 1989; **81**: 742–753.

Hughes GL, Dodson BL, Johnson RM, Murdock CC, Tsujimoto H, Suzuki Y, et al. Native microbiome impedes vertical transmission of *Wolbachia* in *Anopheles* mosquitoes. *Proc Natl Acad Sci* 2014; **111**: 12498-12503.

Jupatanakul N, Sim S, Dimopoulos G. The insect microbiome modulates vector competence for arboviruses. *Viruses* 2014; **6**: 4294–4313.

Kandlikar GS, Gold ZJ, Cowen MC, Meyer RS, Freise AC, Kraft NJB, et al. ranacapa: An R package and Shiny web app to explore environmental DNA data with exploratory statistics and interactive visualizations. *F1000Research* 2018; **7**.

Kindt R. Package ‘ BiodiversityR ’. *R Proj* 2016.

Klindworth A, Pruesse E, Schweer T, Peplies J, Quast C, Horn M, et al. Evaluation of general 16S ribosomal RNA gene PCR primers for classical and next-generation sequencing-based diversity studies. *Nucleic Acids Res* 2013; **41**: e1.

Kraemer MUG, Sinka ME, Duda KA, Mylne AQN, Shearer FM, Barker CM, et al. The global distribution of the arbovirus vectors *Aedes aegypti* and *Ae. Albopictus*. *Elife* 2015; **4**: e08347.

Krishnamoorthy K, Lee M. Improved tests for the equality of normal coefficients of variation. *Comput Stat* 2014; **29**: 215–232.

Lichtwardt RW. Species of Harpellales Living Within the Guts of Aquatic Diptera Larvae. *Mycotaxon* 1984; **19**: 529–550.

Lichtwardt RW. The Trichomycetes: Fungal Associates of Arthropods. Springer-Verlag. New York Inc.; 1986.

Lüdecke D. Sjstats: Statistical Functions for Regression Models. 2017.

Magoč T, Salzberg SL. FLASH: Fast length adjustment of short reads to improve genome assemblies. *Bioinformatics* 2011; **27**: 2957–2963.

Marwick B, Krishnamoorthy K. cvequality: Tests for the Equality of Coefficients of Variation from Multiple Groups. 2016.

McCreadie JW, Beard CE. The microdistribution of the trichomycete *Smittium culisetae* in the hindgut of the black fly host *Simulium vittatum*. *Mycologia* 2003; **95**: 998–1003.

McCreadie JW, Beard CE, Adler PH. Context-dependent symbiosis between black flies (Diptera: Simuliidae) and trichomycete fungi (Harpellales: Legeriomycetaceae). *Oikos* 2005; **108**: 362–370.

McMurdie PJ, Holmes S. Phyloseq: An R Package for Reproducible Interactive Analysis and Graphics of Microbiome Census Data. *PLoS One* 2013; **8**: e61217.

Minard G, Mavingui P, Moro CV. Diversity and function of bacterial microbiota in the mosquito holobiont. *Parasites and Vectors* 2013; **6**: 146–158.

Moll RM, Romoser WS, Modrakowski MC, Moncayo AC, Lerdthusnee K. Meconial Peritrophic Membranes and the Fate of Midgut Bacteria During Mosquito (Diptera: Culicidae) Metamorphosis. *J Med Entomol* 2001; **38**: 29–32.

Moncayo AC, Lerdthusnee K, Leon R, Robich RM, Romoser WS. Meconial Peritrophic Matrix Structure, Formation, and Meconial Degeneration in Mosquito Pupae/Pharate Adults: Histological and Ultrastructural Aspects. *J Med Entomol* 2005; **42**: 939–944.

Muturi EJ, Bara JJ, Rooney AP, Hansen AK. Midgut fungal and bacterial microbiota of *Aedes triseriatus* and *Aedes japonicus* shift in response to La Crosse virus infection. *Mol Ecol* 2016a; **25**: 4075–4090.

Muturi EJ, Kim CH, Bara J, Bach EM, Siddappaji MH. *Culex pipiens* and *Culex restuans* mosquitoes harbor distinct microbiota dominated by few bacterial taxa. *Parasites and Vectors* 2016b; **9**: 18.

Muturi EJ, Ramirez JL, Rooney AP, Kim CH. Comparative analysis of gut microbiota of mosquito communities in central Illinois. *PLoS Negl Trop Dis* 2017; **11**: e0005377.

Novakova E, Woodhams DC, Rodríguez-Ruano SM, Brucker RM, Leff JW, Maharaj A, et al. Mosquito microbiome dynamics, a background for prevalence and seasonality of West Nile virus. *Front Microbiol* 2017; **8**: 526.

Oliveira JHM, Gonçalves RLS, Lara FA, Dias FA, Gandara ACP, Menna-Barreto RFS, et al. Blood meal-derived heme decreases ROS levels in the midgut of *Aedes aegypti* and allows proliferation of intestinal microbiota. *PLoS Pathog* 2011; **7**: e1001320.

Pan X, Zhou G, Wu J, Bian G, Lu P, Raikhel AS, et al. *Wolbachia* induces reactive oxygen species (ROS)-dependent activation of the Toll pathway to control dengue virus in the mosquito Aedes aegypti. *Proc Natl Acad Sci* 2012; **109**: E23–E31.

Pruesse E, Quast C, Knittel K, Fuchs BM, Ludwig W, Peplies J, et al. SILVA: a comprehensive online resource for quality checked and aligned ribosomal RNA sequence data compatible with ARB. *Nucleic Acids Research* 2007; **35**: 7188-7196.

Quast C, Pruesse E, Yilmaz P, Gerken J, Schweer T, Yarza P, et al. The SILVA ribosomal RNA gene database project: Improved data processing and web-based tools. *Nucleic Acids Res* 2013; **41**: D590–D596.

Ramirez JL, Souza-Neto J, Cosme RT, Rovira J, Ortiz A, Pascale JM, et al. Reciprocal tripartite interactions between the *Aedes aegypti* midgut microbiota, innate immune system and dengue virus influences vector competence. *PLoS Negl Trop Dis* 2012; **6**: e1561.

Ramirez JL, Short SM, Bahia AC, Saraiva RG, Dong Y, Kang S, et al. *Chromobacterium* Csp_P Reduces Malaria and Dengue Infection in Vector Mosquitoes and Has Entomopathogenic and In Vitro Anti-pathogen Activities. *PLoS Pathog* 2014; **10**: e1004398.

Ramirez JL, Dunlap CA, Muturi EJ, Barletta ABF, Rooney AP. Entomopathogenic fungal infection leads to temporospatial modulation of the mosquito immune system. *PLoS Negl Trop Dis* 2018; **12**: e0006433.

Rani A, Sharma A, Rajagopal R, Adak T, Bhatnagar RK. Bacterial diversity analysis of larvae and adult midgut microflora using culture-dependent and culture-independent methods in lab-reared and field-collected *Anopheles stephensi*-an Asian malarial vector. *BMC Microbiol* 2009; **9**: 96.

Rizzo AM, Pang K. New primers for detection of *Smittium* spp . (Trichomycetes , Zygomycota) in insect hosts. *Fungal Divers* 2005; **19**: 129–136.

Salter SJ, Cox MJ, Turek EM, Calus ST, Cookson WO, Moffatt MF, et al. Reagent and laboratory contamination can critically impact sequence-based microbiome analyses. *BMC Biol* 2014; **12**: 87.

Schliep KP. phangorn: Phylogenetic analysis in R. *Bioinformatics* 2011; **27**: 592–593.

Sharma P, Sharma S, Maurya RK, De T Das, Thomas T, Lata S, et al. Salivary glands harbor more diverse microbial communities than gut in *Anopheles culicifacies*. *Parasites and Vectors* 2014; **7**: 235.

Sinha R, Abnet CC, White O, Knight R, Huttenhower C. The microbiome quality control project: Baseline study design and future directions. *Genome Biol* 2015; **16**: 276.

Sinha R, Abu-Ali G, Vogtmann E, Fodor AA, Ren B, Amir A, et al. Assessment of variation in microbial community amplicon sequencing by the Microbiome Quality Control (MBQC) project consortium. *Nat Biotechnol* 2017; **35**: 1077–1086.

Smets W, Leff JW, Bradford MA, McCulley RL, Lebeer S, Fierer N. A method for simultaneous measurement of soil bacterial abundances and community composition via 16S rRNA gene sequencing. *Soil Biol Biochem* 2016; **96**: 145–151.

Stämmler F, Gläsner J, Hiergeist A, Holler E, Weber D, Oefner PJ, et al. Adjusting microbiome profiles for differences in microbial load by spike-in bacteria. *Microbiome* 2016; **4**: 28.

Takahashi S, Tomita J, Nishioka K, Hisada T, Nishijima M. Development of a prokaryotic universal primer for simultaneous analysis of Bacteria and Archaea using next-generation sequencing. *PLoS One* 2014; **9**: e105592.

Terenius O, Lindh JM, Eriksson-Gonzales K, Bussière L, Laugen AT, Bergquist H, et al. Midgut bacterial dynamics in *Aedes aegypti*. *FEMS Microbiol Ecol* 2012; **80**: 556–565.

Vojvodic S, McCreadie JW. The effect of temperature and host species on the development of the trichomycete *Smittium culisetae* (Zygomycota). *Mycologia* 2007; **99**: 412–420.

Wang Y, Gilbreath TM, Kukutla P, Yan G, Xu J. Dynamic gut microbiome across life history of the malaria mosquito *Anopheles gambiae* in Kenya. *PLoS One* 2011; **6**: 1–9.

Wei G, Lai Y, Wang G, Chen H, Li F, Wang S. Insect pathogenic fungus interacts with the gut microbiota to accelerate mosquito mortality. *Proc Natl Acad Sci* 2017; **114**: 5994–5999.

Wickham H. Ggplot2. *Wiley Interdiscip Rev Comput Stat* 2011; **3**: 180–185.

Williams MC. Spore Longevity of *Smittium culisetae* (Harpellales , Legeriomycetaceae). *Mycologia* 1983; **75**: 171–174.

Williams MC, Lichtwardt RW. Infection of *Aedes aegypti* larvae by axenic cultures of the fungal genus *Smittium* (Trichomycetes). *Am J Bot* 1972; **59**: 189–193.

Zink SD, van Slyke GA, Palumbo MJ, Kramer LD, Ciota AT. Exposure to west nile virus increases bacterial diversity and immune gene expression in *Culex pipiens*. *Viruses* 2015; **7**: 5619–5631.

Zouache K, Raharimalala FN, Raquin V, Tran-Van V, Raveloson LHR, Ravelonandro P, et al. Bacterial diversity of field-caught mosquitoes, *Aedes albopictus* and *Aedes aegypti*, from different geographic regions of Madagascar. *FEMS Microbiol Ecol* 2011; **75**: 377–389.

APPENDIX A

Supplementary Figures

Paired-end reads for 1 sample from non-fungal larvae (**A**), fungal larvae (**B**), non-fungal adults (**C**), and fungal adults (**D**) treatment groups were merged to assess amplicon lengths prior to read filtering and trimming.

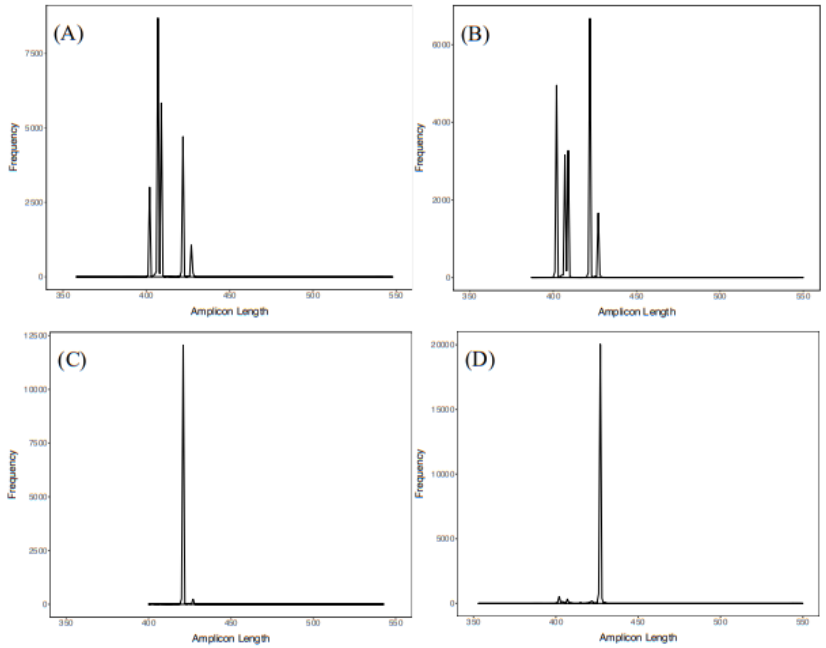

Figure A.1 Amplicon Length Estimates Using FLASH

Rarefaction curves generated for datasets containing reads for larva type (**A**), adult type (**B**), non-fungal mosquitoes (**C**), and fungal mosquitoes (**D**). Rarefaction values used for each dataset are indicated with dashed lines.

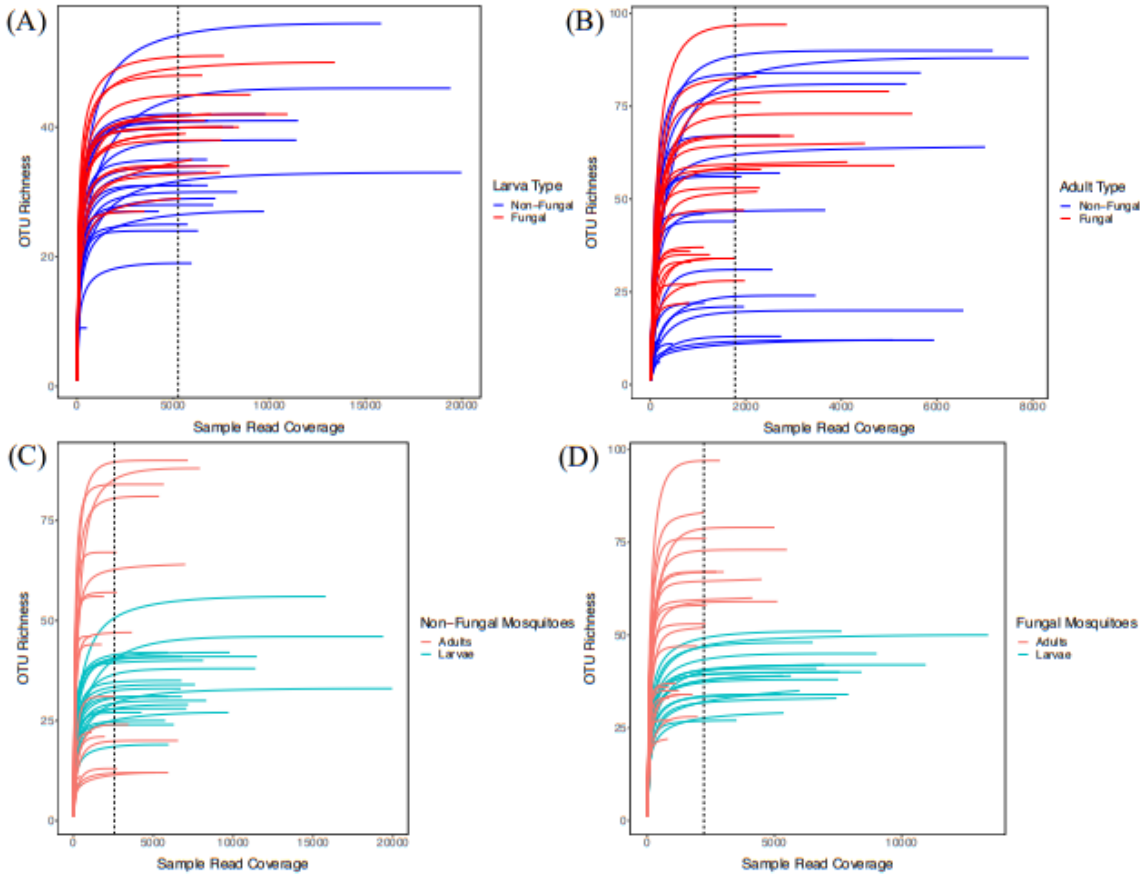

Figure A.2 Dataset Rarefaction Curves

Calibrated read counts for non-fungal and fungal larvae and adults using the SCML method. Error bars represent the standard error. Significant differences in mean calibrated counts across developmental stages within treatments were calculated using linear mixed models and indicated with solid lines black lines labeled with *P<0.05.

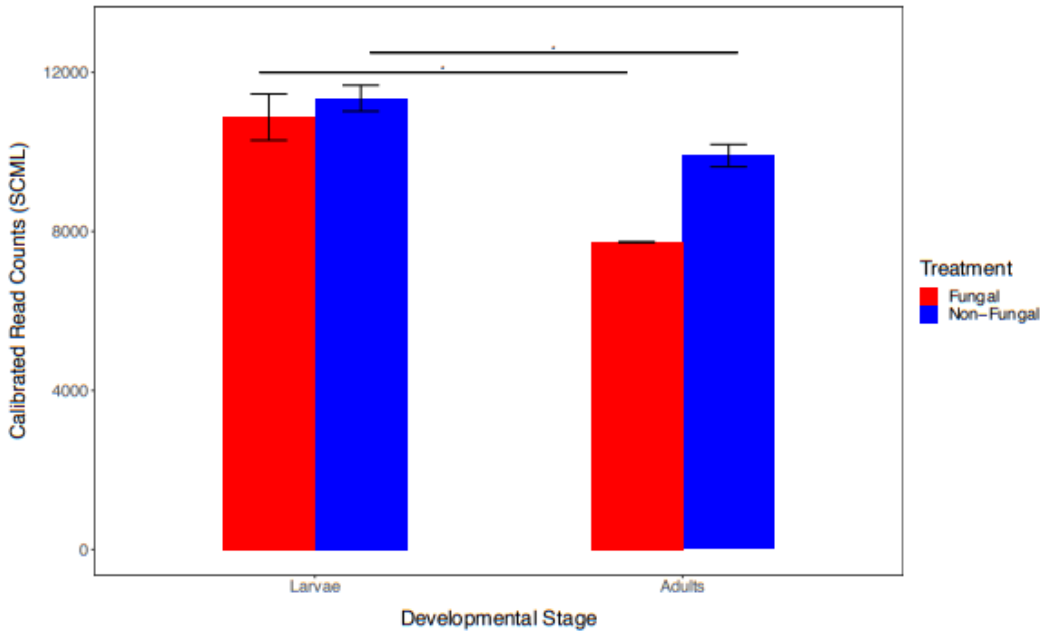

Figure A.3 Bar Plot of SCML Calibrated Read Counts

Relative abundances of the top 15 bacterial families in mosquito eggs (**A**) and the top 15 bacterial families shared in a food sample across 3 days after preparation (**B**). Colored segments in each bar represent different bacterial families and the height of each segment corresponds to the relative percentage of reads assigned to a given family out of the total reads belonging to the top 15 families. Family colors are consistent across all plots.

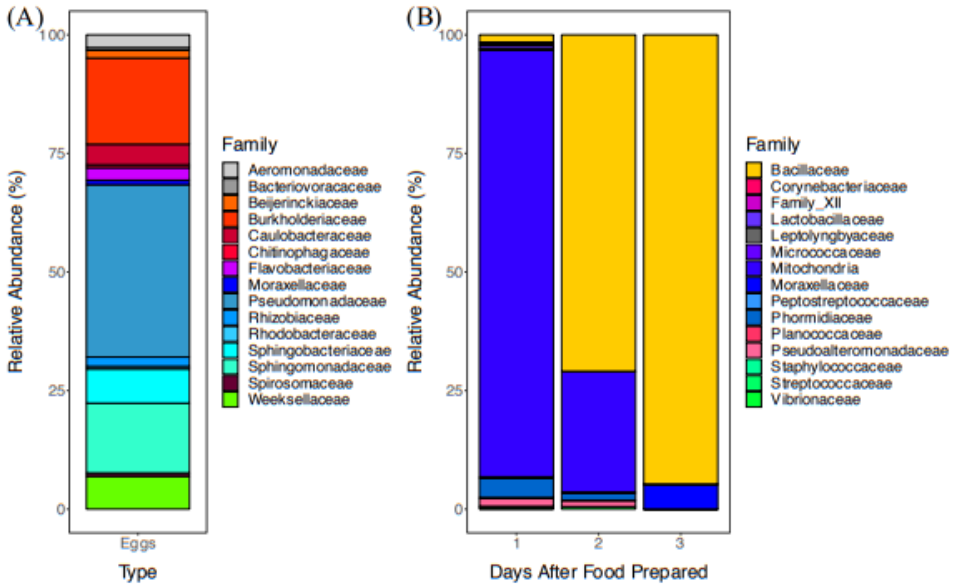

Figure A.4 Bar Plots of the Relative Abundances of Bacterial Families from Positive Controls

APPENDIX B

Supplementary Tables

Table B.1 Supplemental Larval Dissections

Dissections of larvae from each treatment were performed over the course of the experiment to assess fungal infestation in treatments B and D and fungal contamination in treatments A and C. Hindguts were removed and visualized with phase-contrast and Nomarski microscopy and fungal infestation was subjectively quantified.

Treatment	Container	ID	Name	Instar	Date	Infestation Level
A	1	1	A1_1	4	6/15/18	none
A	3	1	A3_1	4	6/15/18	none
A	3	2	A3_2	4	6/15/18	none
A	3	3	A3_3	4	6/15/18	none
A	3	4	A3_4	4	6/15/18	none
A	4	1	A4_1	4	6/15/18	none
A	4	2	A4_2	4	6/15/18	none
A	4	3	A4_3	4	6/16/18	none
B	1	1	B1_1	4	6/10/18	mid
B	1	2	B1_2	4	6/10/18	high
B	1	3	B1_3	4	6/10/18	mid
B	1	4	B1_4	4	6/10/18	mid
B	2	1	B2_1	4	6/10/18	mid
B	2	3	B2_3	4	6/10/18	none
B	3	1	B3_1	3	6/7/18	none
B	3	2	B3_2	4	6/7/18	low
B	3	3	B3_3	4	6/10/18	high
B	3	4	B3_4	4	6/10/18	low
B	3	5	B3_5	4	6/10/18	none
B	4	1	B4_1	4	6/10/18	high
B	4	2	B4_2	4	6/10/18	high
B	4	3	B4_3	4	6/10/18	high
C	2	1	C2_1	4	6/16/18	none
C	2	2	C2_2	4	6/16/18	none
C	2	3	C2_3	4	6/19/18	none
C	3	1	C3_1	4	6/19/18	none
C	3	2	C3_2	4	6/19/18	none
C	3	3	C3_3	4	6/19/18	none
C	4	1	C4_1	4	6/16/18	none
C	4	2	C4_2	4	6/16/18	none
C	4	3	C4_3	4	6/19/18	none

D	1	1	D1_1	3	6/7/18	none
D	1	2	D1_2	3	6/7/18	none
D	1	3	D1_3	4	6/10/18	high
D	1	4	D1_4	4	6/10/18	high
D	1	5	D1_5	4	6/10/18	high
D	1	6	D1_6	4	6/19/18	high
D	2	1	D2_1	4	6/10/18	high
D	2	2	D2_2	4	6/10/18	high
D	2	3	D2_3	4	6/10/18	none
D	3	1	D3_1	4	6/10/18	none
D	3	2	D3_2	4	6/15/18	none
D	3	3	D3_3	4	6/16/18	none
D	4	1	D4_1	4	6/10/18	mid
D	4	2	D4_2	4	6/10/18	none
D	4	3	D4_3	4	6/10/18	high

Table B.2 Primer Sequences

Primer ID	Paired ID	Spacer	Linker	Primer Sequence
341f_1	785r_1	.	AG	CCTACGGGNGGCWGCAG
341f_2	785r_2	T	AG	CCTACGGGNGGCWGCAG
341f_3	785r_3	CT	AG	CCTACGGGNGGCWGCAG
341f_4	785r_4	GCT	AG	CCTACGGGNGGCWGCAG
785r_1	341f_1	.	CT	GACTACHVGGGTATCTAATCC
785r_2	341f_2	T	CT	GACTACHVGGGTATCTAATCC
785r_3	341f_3	AT	CT	GACTACHVGGGTATCTAATCC
785r_4	341f_4	GAT	CT	GACTACHVGGGTATCTAATCC
TR3	TR4	.	.	GGCACTGTCAGTGGTGAAATAC
TR4	TR3	.	.	GATTTCTCTTACGGTGCCAAGCA

Table B.3 PCR Setup

ID	Total (ul)	Primer ID	Master Mix (ul)	10uM Primer (ul)	Template DNA (ul)	*S. ruber* DNA (ul)	Nuclease Free H_2O (ul)
Rxn_1	50	TR3-TR4	20	2	2	.	26
Rxn_2	50	341f-785r	20	2	2	.	26
Rxn_3	50	341f-785r	20	2	2	0.59	25.41
Rxn_4	25	Barcodes	10	0.94	1.25	.	12.81

Table B.4 PCR Thermocycler Settings

ID	Initial Denaturation	Duration (min)	Denaturation	Duration (min)	Annealing	Duration (min)	Elongation	Duration (min)	Cycles	Final Elongation	Duration (min)
Rxn_1	95°C	2	95°C	1	55°C	1.5	72°C	1.5	35	72°C	10
Rxn_2	94°C	3	94°C	0.75	60°C	1	72°C	1.5	35	72°C	10
Rxn_3	94°C	3	94°C	0.75	60°C	1	72°C	1.5	35	72°C	10
Rxn_4	94°C	1.5	94°C	0.5	60°C	0.5	72°C	1.5	10	72°C	5

Table B.5 Experimental Sample Read Counts

Total read counts for experimental samples throughout the DADA2 pipeline. Raw reads (Input) were filtered based on quality filtering thresholds (Filtered). After filtering and merging, chimeric sequences were removed (Final). Final reads were used in downstream analyses.

Sample ID	Larva Type	Input Reads	Filtered Reads	Final Reads
A1i16S	Non-Fungal	30503	10305	8357
A1ii16S	Non-Fungal	19731	6740	5748
A1iii16S	Non-Fungal	33025	7649	5957
A1IV16S	Non-Fungal	36177	9725	7204
A1V16S	Non-Fungal	26734	8669	7098
A1VI16S	Non-Fungal	34814	12025	9730
A2i16S	Non-Fungal	21713	7768	6302
A2ii16S	Non-Fungal	26364	6029	4256
A2iii16S	Non-Fungal	102021	22260	15857
A2IV16S	Non-Fungal	55246	16159	11399
A2V16S	Non-Fungal	40984	9423	6821
A3i16S	Non-Fungal	28682	7772	5954
A3ii16S	Non-Fungal	53382	14702	11516
A3iii16S	Non-Fungal	31690	9696	6765
A3IV16S	Non-Fungal	48438	13459	9789
A3V16S	Non-Fungal	2247	607	517
A3VI16S	Non-Fungal	46631	11336	8161
A4i16S	Non-Fungal	36206	8915	6729
A4ii16S	Non-Fungal	30948	8624	6792
A4iii16S	Non-Fungal	108466	23371	19406
A4IV16S	Non-Fungal	82115	23930	19977
A4V16S	Non-Fungal	33193	8718	5938
A4VI16S	Non-Fungal	33683	10501	7613
B1i16S	Fungal	17910	6007	5251
B1ii16S	Fungal	23021	7937	6961
B1iii16S	Fungal	32738	7753	5658
B1V16S	Fungal	38019	9730	6653
B1VII16S	Fungal	23064	5001	3510
B1XI16S	Fungal	28316	8634	6550
B2iii16S	Fungal	26605	7894	6014
B2V16S	Fungal	31523	9362	7469

B2VII16S	Fungal	37173	9224	7727
B2VIII16S	Fungal	23434	6669	5354
B2XII16S	Fungal	73279	17003	13436
B3iii16S	Fungal	45081	10832	8416
B3IV16S	Fungal	35372	10344	7908
B3V16S	Fungal	34849	9726	7556
B3VI16S	Fungal	33090	9984	7498
B3VIII16S	Fungal	44932	12346	9028
B4i16S	Fungal	27720	6869	5383
B4X16S	Fungal	73456	13836	11032
	Adult Type			
C1i16S	Non-Fungal	30959	2477	2225
C1ii16S	Non-Fungal	61070	8192	7452
C1iii16S	Non-Fungal	33209	6741	6007
C1IV16S	Non-Fungal	34877	2752	2248
C1V16S	Non-Fungal	9685	1583	1312
C1VI16S	Non-Fungal	46577	7530	6787
C2i16S	Non-Fungal	37258	9438	8379
C2ii16S	Non-Fungal	22263	6756	5973
C2iii16S	Non-Fungal	15165	3812	3533
C2IV16S	Non-Fungal	52548	4585	4168
C2V16S	Non-Fungal	20136	6995	6553
C3i16S	Non-Fungal	18369	3347	3050
C3ii16S	Non-Fungal	57055	8448	7585
C3iii16S	Non-Fungal	19861	5466	5094
C3IV16S	Non-Fungal	44140	1825	1309
C3VI16S	Non-Fungal	23932	404	212
C4i16S	Non-Fungal	18620	2891	2658
C4ii16S	Non-Fungal	40259	3056	2770
C4iii16S	Non-Fungal	13488	2417	2212
C4IV16S	Non-Fungal	34615	3482	3127
C4V16S	Non-Fungal	19444	644	481
C4VI16S	Non-Fungal	24502	544	257
C4VII16S	Non-Fungal	19332	421	193
D1i16S	Fungal	27012	1298	929
D1ii16S	Fungal	31538	1392	971
D1iii16S	Fungal	11703	1929	1437

D1IV16S	Fungal	8248	2793	2499
D2i16S	Fungal	32813	6026	5538
D2ii16S	Fungal	16159	2380	2043
D2iii16S	Fungal	26063	2967	2564
D2IV16S	Fungal	35618	3587	2908
D2V16S	Fungal	40220	3914	3044
D2VI16S	Fungal	6469	2324	1951
D3i16S	Fungal	19160	4008	3456
D3ii16S	Fungal	12151	2861	2371
D3iii16S	Fungal	32827	6044	5488
D3IV16S	Fungal	15892	3213	2727
D3V16S	Fungal	36320	5848	5268
D3VI16S	Fungal	20009	1150	848
D4i16S	Fungal	39065	2879	2274
D4ii16S	Fungal	37759	1747	1197
D4iii16S	Fungal	32686	6791	6012
D4IV16S	Fungal	18234	3285	2562
D4V16S	Fungal	33153	2334	1453
D4VI16S	Fungal	18120	6030	5425
D4VII16S	Fungal	26429	1620	987
	SCML Larva Type			
A1ia16S	Non-Fungal	17706	5675	5222
A1iia16S	Non-Fungal	49012	12740	11276
A2ia16S	Non-Fungal	124337	32007	28200
A2iia16S	Non-Fungal	14921	4854	4448
A3ia16S	Non-Fungal	15794	3878	3567
A3iia16S	Non-Fungal	27801	6744	6440
A4ia16S	Non-Fungal	87100	18955	17793
A4iia16S	Non-Fungal	26875	6668	5807
B1ia16S	Fungal	56789	13665	12983
B1iia16S	Fungal	79438	18647	18064
B1iiia16S	Fungal	45785	8848	8394
B1Va16S	Fungal	26276	8417	7200
B1VIIa16S	Fungal	30284	8925	8227
B1XIa16S	Fungal	25337	7267	6695
B2iiia16S	Fungal	14585	4238	3856
B2Va16S	Fungal	19949	6340	5809

B2VIIa16S	Fungal	25744	8146	7682
B2VIIIa16S	Fungal	32858	10232	9433
B2XIIa16S	Fungal	21277	6355	5613
B3iiia16S	Fungal	25045	8407	7313
B3IVa16S	Fungal	29793	9671	8145
B3Va16S	Fungal	19758	6117	5386
B3VIa16S	Fungal	30488	9790	8272
B3VIIIa16S	Fungal	14770	4683	3985
B4ia16S	Fungal	23375	8020	7012
B4Xa16S	Fungal	40529	12130	10999
	SCML Adult Type			
C1ia16S	Non-Fungal	88981	24380	24213
C1iia16S	Non-Fungal	26604	7777	7709
C2ia16S	Non-Fungal	15067	5515	5422
C2iia16S	Non-Fungal	21511	6858	6430
C3ia16S	Non-Fungal	38792	10976	10893
C3iia16S	Non-Fungal	28146	8102	8030
C4ia16S	Non-Fungal	38257	11681	11560
C4iia16S	Non-Fungal	32408	9438	9349
D1ia16S	Fungal	25051	8740	8676
D1iia16S	Fungal	23889	7357	7279
D2ia16S	Fungal	30855	9766	9698
D2iia16S	Fungal	20892	6400	6342
D3ia16S	Fungal	34257	9759	9653
D3iia16S	Fungal	35003	9362	9221
D4ia16S	Fungal	66826	18787	18649
D4iia16S	Fungal	67662	19755	19574
	Control Type			
FT2216S	Pupa Tube Water	20809	155	50
FT3116S	Pupa Tube Water	12631	174	85
KB016S	Extraction Kit	13731	139	59
KB116S	Extraction Kit	14243	204	112
KB216S	Extraction Kit	11619	241	173
KB316S	Extraction Kit	17370	400	272
SP1316S	Spore Inoculum	15918	152	32
SW16S	Autoclaved Spring Water	18466	128	30

EE16S	50 Mosquito Eggs	38341	14352	10633
FD116S	Fish Slurry	43325	7940	7142
FD216S	Fish Slurry 1 Day After Preparation	25570	8925	8188
FD316S	Fish Slurry 2 Days After Preparation	31533	12613	12379

Table B.6 Measures of Alpha Diversity and Coefficient of Variation Values

Measures of alpha diversity, CV values, and results from statistical analyses on group means and variation of measures. *P* (Treatment or Developmental Stage) values were calculated with linear mixed models. CV *P* values were calculated with an asymptotic test and MSLRT. Significant *P* values are shown in bold text.

Dataset	Metric	F Value	*P* (Treatment)	Non-Fungal CV	Fungal CV	CV *P* (Combined)
Larva Type	Simpson	0.798	0.406	9.02%	5.91%	<0.1
Larva Type	Shannon	1.941	0.214	17.65%	11.77%	<0.1
Adult Type	Simpson	4.039	0.091	39.64%	8.42%	**<0.001**
Adult Type	Shannon	3.277	0.120	54.45%	17.76%	**<0.001**
			P **(Developmental Stage)**	**Larval CV**	**Adult CV**	**CV *P* (Combined)**
Non-Fungal Mosquitoes	Simpson	1.4683	0.271	9.02%	39.64%	**<0.001**
Non-Fungal Mosquitoes	Shannon	0.0063	0.939	17.65%	54.45%	**<0.001**
Fungal Mosquitoes	Simpson	3.227	0.127	5.91%	8.42%	<0.14
Fungal Mosquitoes	Shannon	13.903	**0.011**	11.77%	17.76%	<0.1

Table B.7 Measures of Beta Diversity and Group Dispersals

Measures of beta diversity and results from statistical analyses on group centroids and variation of measures. Pseudo-F and *P* (Treatment or Developmental Stage) values were calculated with nested PERMANOVA. *P* (Homogeneity) values were calculated using permutational tests of dispersal homogeneity between groups. Significant *P* values are shown in bold text.

Dataset	Metric	Pseudo-F	*P* (Treatment)	F	*P* (Homogeneity)
Larva Type	Bray-Curtis	1.0415	0.442	0.5369	0.489
Larva Type	Unweighted UniFrac	1.0848	0.359	4.6534	**0.036**
Larva Type	Weighted UniFrac	0.977	0.442	0.2971	0.544
Adult Type	Bray-Curtis	1.7003	0.088	2.7112	0.1
Adult Type	Unweighted UniFrac	1.506	0.08	0.8596	0.383
Adult Type	Weighted UniFrac	5.6849	0.05 .	0.0351	0.864
			P **(Developmental Stage)**		
Non-Fungal Mosquitoes	Bray-Curtis	3.7052	**0.022**	31.461	**<0.001**
Non-Fungal Mosquitoes	Unweighted UniFrac	6.9677	**0.035**	43.821	**<0.001**
Non-Fungal Mosquitoes	Weighted UniFrac	8.9194	**0.031**	0.0523	0.824
Fungal Mosquitoes	Bray-Curtis	6.2994	**0.028**	32.067	**<0.001**
Fungal Mosquitoes	Unweighted UniFrac	10.7434	**0.03**	53.22	**<0.001**
Fungal Mosquitoes	Weighted UniFrac	8.4334	**0.025**	0.2496	0.632

Table B.8 Relative Abundances of Bacterial Families

Relative abundances and results from statistical analyses on group means of the top 15 bacterial families shared between groups in each dataset. *P* (Treatment or Developmental Stage) values were calculated with linear mixed models. Significant *P* values are shown in bold text.

Dataset	Family	Relative Abundance (Non-Fungal)	Relative Abundance (Fungal)	*P* (Treatment)
Larva Type	Bacillaceae	0.10%	9.55%	0.348
Larva Type	Bdellovibrionaceae	0.55%	1.66%	0.152
Larva Type	Beijerinckiaceae	2.10%	1.47%	0.514
Larva Type	Burkholderiaceae	2.24%	10.18%	0.219
Larva Type	Caulobacteraceae	0.46%	0.84%	0.253
Larva Type	Chitinophagaceae	6.50%	2.05%	0.433
Larva Type	Enterobacteraceae	0.69%	1.46%	0.466
Larva Type	env.OPS_17	0.01%	1.73%	0.146
Larva Type	Flavobacteriaceae	0.03%	4.41%	0.348
Larva Type	Microbacteriaceae	49.98%	29.41%	0.177
Larva Type	Pseudomonadaceae	2.74%	5.56%	0.178
Larva Type	Rhizobiaceae	10.11%	8.42%	0.548
Larva Type	Sphingobacteriaceae	8.21%	9.59%	0.792
Larva Type	Sphingomonadaceae	0.72%	1.22%	0.428
Larva Type	Weeksellaceae	12.74%	8.92%	0.646
Adult Type	Burkholderiaceae	40.19%	10.44%	0.077
Adult Type	Corynebacteriaceae	4.08%	12.58%	**0.025**
Adult Type	Enterobacteriaceae	6.14%	1.23%	0.413
Adult Type	Family_XI	2.10%	4.92%	0.065
Adult Type	Geodermatophilaceae	1.53%	1.25%	0.978
Adult Type	Lactobacillaceae	0.99%	0.97%	0.987
Adult Type	Microbacteriaceae	0.23%	2.78%	0.363
Adult Type	Micrococcaceae	2.16%	4.60%	0.398
Adult Type	Moraxellaceae	1.31%	3.91%	**0.048**
Adult Type	Pseudomonadaceae	8.12%	4.27%	0.483
Adult Type	Rhizobiaceae	1.22%	1.32%	0.891
Adult Type	Rhodobacteraceae	0.84%	1.58%	0.335
Adult Type	Sphingomonadaceae	1.80%	2.12%	0.808
Adult Type	Staphylococcaceae	7.16%	18.57%	0.054
Adult Type	Streptococcaceae	1.77%	2.99%	0.301
		Relative Abundance (Larvae)	**Relative Abundance (Adults)**	***P*** **(Developmental Stage)**

Non-Fungal Mosquitoes	Beijerinckiaceae	2.10%	0.38%	0.144
Non-Fungal Mosquitoes	Burkholderiaceae	2.23%	42.16%	**0.002**
Non-Fungal Mosquitoes	Chitinophagaceae	6.29%	0.27%	0.259
Non-Fungal Mosquitoes	Corynebacteriaceae	0.01%	3.32%	**0.007**
Non-Fungal Mosquitoes	Enterobacteriaceae	0.99%	6.53%	0.316
Non-Fungal Mosquitoes	Family_XI	0.01%	2.29%	**0.042**
Non-Fungal Mosquitoes	Microbacteriaceae	49.47%	0.30%	**0.002**
Non-Fungal Mosquitoes	Moraxellaceae	0.22%	1.25%	**0.012**
Non-Fungal Mosquitoes	Pseudomonadaceae	2.68%	8.69%	0.254
Non-Fungal Mosquitoes	Rhizobiaceae	10.26%	1.28%	**0.015**
Non-Fungal Mosquitoes	Rhodobacteraceae	0.41%	1.06%	0.192
Non-Fungal Mosquitoes	Sphingobacteriaceae	8.79%	0.11%	0.115
Non-Fungal Mosquitoes	Sphingomonadaceae	0.64%	1.27%	0.339
Non-Fungal Mosquitoes	Staphylococcaceae	0.02%	7.15%	**0.044**
Non-Fungal Mosquitoes	Weeksellaceae	12.66%	0.42%	0.103
Fungal Mosquitoes	Bacillaceae	9.09%	0.64%	0.382
Fungal Mosquitoes	Burkholderiaceae	9.57%	5.59%	0.511
Fungal Mosquitoes	Corynebacteriaceae	0.02%	12.05%	**0.002**
Fungal Mosquitoes	Enterobacteriaceae	1.34%	1.48%	0.650
Fungal Mosquitoes	Family_XI	0.01%	5.05%	**0.001**
Fungal Mosquitoes	Flavobacteriaceae	4.33%	0.14%	0.374
Fungal Mosquitoes	Microbacteriaceae	31.26%	3.32%	**0.013**
Fungal Mosquitoes	Micrococcaceae	0.00%	4.98%	0.101
Fungal Mosquitoes	Moraxellaceae	0.26%	4.44%	**0.010**
Fungal Mosquitoes	Pseudomonadaceae	5.35%	5.06%	0.941
Fungal Mosquitoes	Rhizobiaceae	8.23%	1.61%	**0.013**
Fungal Mosquitoes	Sphingobacteriaceae	9.91%	0.18%	**0.007**
Fungal Mosquitoes	Sphingomonadaceae	1.28%	2.31%	0.098
Fungal Mosquitoes	Staphylococcaceae	0.07%	18.49%	**0.003**
Fungal Mosquitoes	Weeksellaceae	8.67%	0.12%	0.150

Table B.9 SCML Calibrated Read Counts

Total reads for experimental samples spiked with *Salinibacter ruber* DNA, the number of reads belonging to *S. ruber*, calibrated read counts using the SCML method, and results of statistical analyses comparing SCML calibrated read counts across developmental stages within treatments. *P* (Developmental Stage) values were calculated using linear mixed models. Significant *P* values are shown in bold text.

Sample ID	Treatment	Developmental Stage	Total Reads	*S.ruber* Reads	SCML Reads
A1ia16S	Non-Fungal	Larvae	5222	4256	11741
A1iia16S	Non-Fungal	Larvae	11276	9511	11345
A2ia16S	Non-Fungal	Larvae	28200	24148	11175
A2iia16S	Non-Fungal	Larvae	4448	3370	12630
A3ia16S	Non-Fungal	Larvae	3567	3176	10747
A3iia16S	Non-Fungal	Larvae	6440	6184	9965
A4ia16S	Non-Fungal	Larvae	17793	15974	10659
A4iia16S	Non-Fungal	Larvae	5807	4439	12518
C1ia16S	Non-Fungal	Adults	24213	24213	9569
C1iia16S	Non-Fungal	Adults	7709	7697	9584
C2ia16S	Non-Fungal	Adults	5422	5334	9727
C2iia16S	Non-Fungal	Adults	6430	5184	11869
C3ia16S	Non-Fungal	Adults	10893	10893	9569
C3iia16S	Non-Fungal	Adults	8030	7993	9613
C4ia16S	Non-Fungal	Adults	11560	11452	9659
C4iia16S	Non-Fungal	Adults	9349	9280	9640
B1ia16S	Fungal	Larvae	12983	11945	8379
B1iia16S	Fungal	Larvae	18064	17338	8032
B1iiia16S	Fungal	Larvae	8394	7927	8163
B1Va16S	Fungal	Larvae	7200	4836	11477
B1VIIa16S	Fungal	Larvae	8227	6913	9174
B1XIa16S	Fungal	Larvae	6695	5564	9276
B2iiia16S	Fungal	Larvae	3856	3175	9362
B2Va16S	Fungal	Larvae	5809	4380	10224
B2VIIa16S	Fungal	Larvae	7672	6790	8710
B2VIIIa16S	Fungal	Larvae	9433	7824	9294
B2XIIa16S	Fungal	Larvae	5613	4244	10196
B3iiia16S	Fungal	Larvae	7313	3859	14609
B3IVa16S	Fungal	Larvae	8145	4129	15207
B3Va16S	Fungal	Larvae	5386	3434	12091

B3VIa16S	Fungal	Larvae	8272	4104	15538
B3VIIIa16S	Fungal	Larvae	3985	2268	13545
B4ia16S	Fungal	Larvae	7003	4371	12351
B4Xa16S	Fungal	Larvae	10999	8427	10062
D1ia16S	Fungal	Adults	8676	8673	7712
D1iia16S	Fungal	Adults	7279	7272	7716
D2ia16S	Fungal	Adults	9693	9670	7727
D2iia16S	Fungal	Adults	6342	6301	7759
D3ia16S	Fungal	Adults	9653	9638	7721
D3iia16S	Fungal	Adults	9221	9174	7748
D4ia16S	Fungal	Adults	18649	18642	7712
D4iia16S	Fungal	Adults	19574	19532	7725
Dataset	**DF Num**	**DF Den**	**F Value**	***P*** **(Developmental Stage)**	
Non-Fungal Mosquitoes	1	6	10.183	**0.019**	
Fungal Mosquitoes	1	6	6.974	**0.038**	